



RESEARCH ARTICLE

WILEY

Sedimentology of a distributive fluvial system: The Serra da Galga Formation, a new lithostratigraphic unit (Upper Cretaceous, Bauru Basin, Brazil)

Marcus Vinícius Theodoro Soares¹  | Giorgio Basilici^{1,2}  |
 Thiago da Silva Marinho^{3,4} | Agustín Guillermo Martinelli⁵ | André Marconato⁶ |
 Nigel Philip Mountney⁷ | Luca Colombero⁷ | Áquila Ferreira Mesquita¹ |
 Julia Tucker Vasques¹ | Francisco Romero Abrantes Junior¹ | Luiz Carlos Borges Ribeiro⁴

¹Department of Geology and Natural Resources, Institute of Geosciences, State University of Campinas, Campinas, Brazil

²Centro Regional de Investigaciones Científicas y Transferencia Tecnológica (CRILAR), Consejo Nacional de Investigaciones Científicas y Técnicas (CONICET), La Rioja, Sao Paulo, Argentina

³Instituto de Ciências Exatas, Naturais e Educação (ICENE), Universidade Federal do Triângulo Mineiro, Uberaba, Minas Gerais, Brazil

⁴Centro de Pesquisas Paleontológicas Llewellyn Ivor Price (CPPLIP), Universidade Federal do Triângulo Mineiro, Uberaba, Minas Gerais, Brazil

⁵Sección Paleontología de Vertebrados, Museo Argentino de Ciencias Naturales 'Bernardino Rivadavia', Consejo Nacional de Investigaciones Científicas y Técnicas (CONICET), Buenos Aires, Argentina

⁶Department of Geology, Federal University of Ouro Preto, Ouro Preto, Brazil

⁷School of Earth and Environment, Fluvial & Eolian Research Group, University of Leeds, Leeds, UK

Correspondence

Marcus Vinícius Theodoro Soares, Institute of Geosciences, State University of Campinas, 13083-870, Campinas, Brazil.
 Email: soares.mvt@gmail.com

Funding information

Conselho Nacional de Desenvolvimento Científico e Tecnológico, Grant/Award Numbers: 305098/2018-7, 310164/2015-0, 474227/2013-8; Fundação de Amparo à Pesquisa do Estado de Minas Gerais, Grant/Award Number: APQ-02194-15; Fundação de Amparo à Pesquisa do Estado de São Paulo, Grant/Award Numbers: 2012/23209-0, 2018/10574-8

The Bauru Basin of SE Brazil is a large (ca. 370,000 km²) Upper Cretaceous intra-cratonic feature, important for its fossil remains and of particular value as a source of regional palaeoclimatic information. Historically, lithostratigraphic reconstructions have been performed mainly for successions of the central and southern parts of the basin, resulting in a lithostratigraphic scheme that is not applicable to the northernmost regions. In particular, the northeastern deposits of the Marília Formation (Serra da Galga and Ponte Alta members) reveal lithological, stratigraphic, and palaeontological differences from southeastern and northwestern counterparts (Echaporã Member). Nevertheless, these deposits are considered as a single lithostratigraphic formation in the literature. To address this problem, this study demonstrates how the northeastern deposits of the Marília Formation do not show affinity to the rest of the unit. A more suitable lithostratigraphic model is proposed for the northeastern succession as a distinct and independent unit. Lithofacies and palaeopedological analysis, combined with lithostratigraphic mapping of the northeastern deposits, reveal 11 distinct lithofacies and three pedotypes over an area of ~450 km². Sedimentary facies and pedotypes were assigned to six interbedded architectural elements: (a) type 1 channel fill, (b) type 2 channel fill, (c) type 3 channel fill, (d) interchannels, (e) palaeosols, and (f) calcrete beds. The succession is interpreted as a distributive fluvial system with overall direction of flow to the NNW, and which developed under the influence of a semiarid climate regime. This contrasts with deposits of the southeastern and northwestern Marília Formation, previously suggested to be of fine-grained aeolian affinity with interbedded poorly channelised deposits assigned to an aeolian sand sheet environment. By revising the existing lithostratigraphic scheme for the northeastern deposits, and contrasting them with laterally equivalent strata, this work demonstrates how the previously named Serra da Galga and Ponte Alta members reveal a unique set of lithological, architectural, and genetic signatures that permits to separate them from the Marília Formation. Finally, a new lithostratigraphic classification for the unit is proposed: the Serra da Galga Formation, whose deposition relates to an ancient distributive fluvial system.

Handling Editor: A. Ruffell

KEYWORDS

Bauru Group, distributive fluvial system, facies, lithostratigraphy, Marília Formation, palaeosols, Serra da Galga Formation

1 | INTRODUCTION

The stratigraphic record of sedimentary basins is traditionally organized and classified through the use of lithostratigraphy (Murphy & Salvador, 1999). This widely accepted approach is essentially descriptive, and is a cornerstone of stratigraphic methodology; it is further used as the basis for understanding the genetic significance of stratigraphic units (Fregenal-Martínez, Meléndez, Muñoz-García, Elez, & Horra, 2017). Although lithostratigraphic subdivisions are commonly grounded exclusively on lithological differences (Murphy & Salvador, 1999), many deposits cannot be distinguished solely by lithological features and stratigraphic position alone (e.g., Schokker, Weerts, Westerhoff, Berendsen, & Otter, 2007). When lithological characteristics of a sedimentary succession are too similar, more detailed approaches are required in order to work out the geologic history of a certain region (Murphy & Salvador, 1999), notably facies analysis and architectural element analysis (cf. Brookfield, 1977; Miall, 1978, 1985). These methods permit (a) establishment of criteria by which to distinguish sedimentary successions (sedimentary structures, geometry, and relationships of bedding and recognition of sedimentary sequences), beyond the simple lithology, and (b) interpretation of the geological history of the region, which is considered to be the foundation of stratigraphy (Rodgers, 1954).

In this regard, the stratigraphy of the Bauru Basin has been investigated since the first half of the 20th century (Washburne, 1930; see Basilici, Sgarbi, & Dal Bó, 2012 for an historical stratigraphic synthesis). However, due to its large extent, and the absence of detailed sedimentological analyses, many stratigraphic schemes have failed to grasp important lithological variations that should be considered for geological mapping purposes, and which therefore should be assigned to the rank of 'formation'. As a consequence, the current stratigraphic framework is not suitable for all areas of the Bauru Basin, since it does not resolve important palaeodepositional and palaeoenvironmental aspects of its geologic history. In particular, the uppermost portion of the infill of the Bauru Basin is traditionally known as the Marília Formation (Barcelos, 1984; Soares, Landim, Fulfaro, & Sobreiro Neto, 1980; see below for stratigraphic details). This unit is present from south to north in the eastern part of the Bauru Basin (Figure 1a) and records deposition in several different depositional environments (Basilici, Fiorelli, & Dal' Bo, 2016; Soares et al., 2018).

Initial studies of the Marília Formation focused on the south-central part of the basin. Here, the stratotype section was defined as constituted by very fine- to fine-grained sandstones, and scarce conglomerates and mudstones (Soares et al., 1980). Later, the recognition of this unit was progressively expanded northwards to the margins of the basin, where the same lithological characteristics were recognized.

However, recent studies (Soares et al., 2018) reveal that the Marília Formation at the northeastern margin of the Bauru Basin displays sedimentary structures and depositional architecture that differ considerably from what is described as the 'same' unit in the southeast part of the Bauru Basin. For this reason, the aim of this study is to revise the stratigraphic organization of the NE Bauru Basin, as a way to associate the depositional characteristics encountered in this area to a plausible stratigraphic context. Specific research objectives are as follows: the in-depth (a) sedimentological, (b) palaeopedological, and (c) architectural characterization of deposits, as well as (d) the geological mapping of the northeastern part of the Bauru Basin; the Serra da Galga Formation is here proposed as a new stratigraphic unit.

2 | GEOLOGICAL SETTING

The Bauru Basin is an intracratonic sedimentary basin that occupies an area of c. 370,000 km² and is filled with ca. 400 m thickness of siliciclastic deposits. The basin evolved from the Coniacian to the Maastrichtian, based on biostratigraphic information (Dias-Brito et al., 2001) and absolute dating of igneous intrusions close to the margins of the basin (Coutinho, Coimbra, Brandt Neto, & Rocha, 1982). During this period, the climate in the Bauru Basin was mostly warm and dry, but with some humid phases (Arai & Dias-Brito, 2018).

Basin-scale stratigraphic characterizations of the Bauru Basin include those of Washburne (1930), Almeida and Barbosa (1953), and Soares et al. (1980). The authors recognized four lithostratigraphic units, from the base to the top: the Caiuá, Santo Anastácio, Adamantina, and Marília formations. Fernandes (1992) and Fernandes and Coimbra (1994) reorganized the previous stratigraphic model of the Bauru Basin and further separated the basin succession into two groups: the Caiuá Group and the Bauru Group, the latter occurring towards the eastern part of the homonymous basin, where more humid climatic conditions prevailed. Several different perspectives on the stratigraphic organization of the Bauru Basin are proposed by other authors (Fulfaro, Etchebehere, Perinotto, & Saad, 1999; Paula e Silva, Chang, & Caetano-Chang, 2003, 2005, 2009; Paula e Silva, Chang, Caetano-Chang, & Stradioto, 2006) although they are in part similar to the earlier model of Soares et al. (1980). However, due to the large extent of the basin, these prior published studies have demonstrated that the stratigraphic organization of the Bauru Basin is rather complex, and general agreement on its formalization is lacking, in particular for the uppermost part of the Bauru Group (Marília Formation).

The Bauru Group is formed by the vertically superposed Araçatuba, Uberaba, Adamantina, and Marília formations (Figure 1).

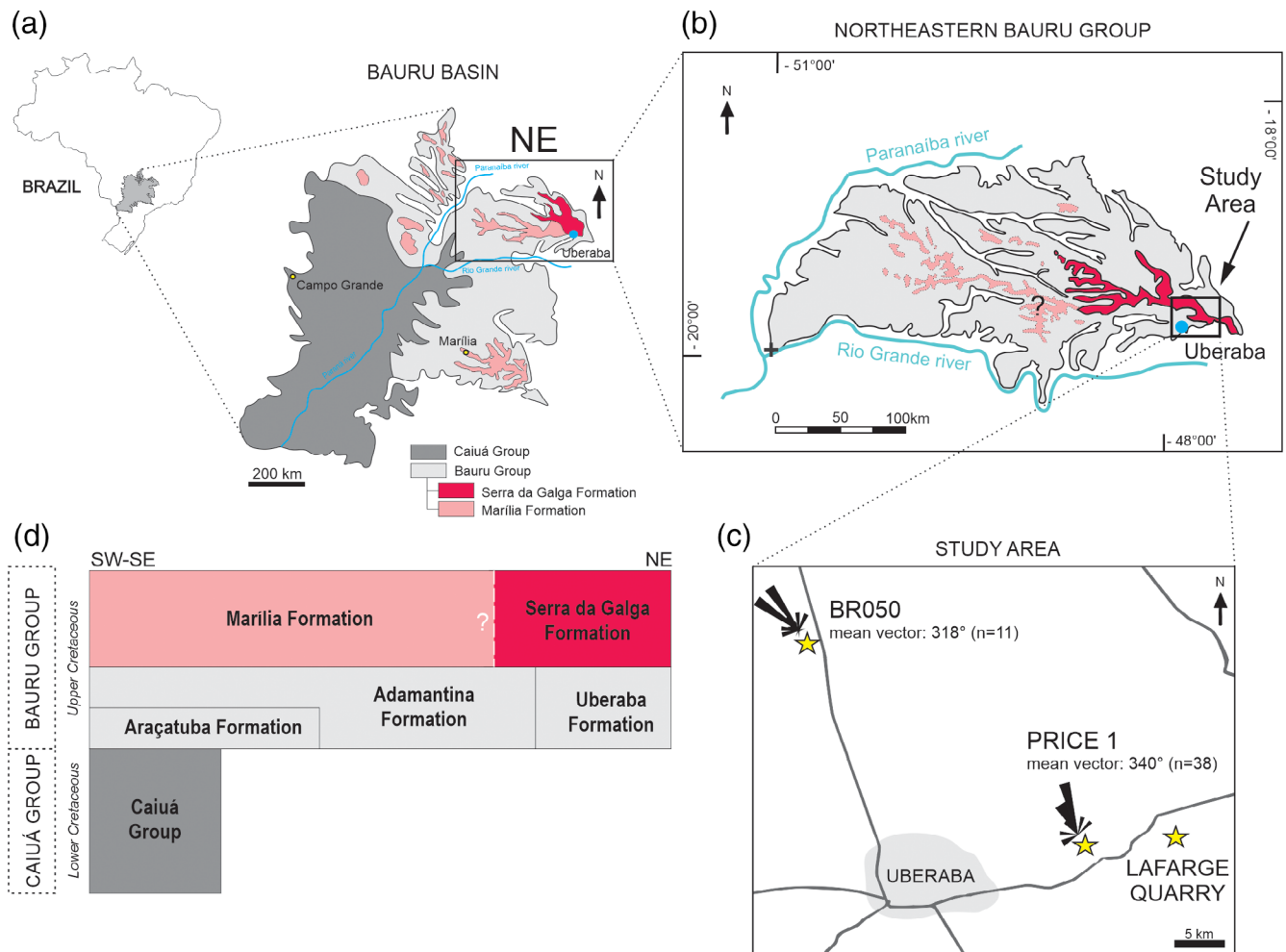


FIGURE 1 (a) Lithostratigraphic map of the Bauru Basin showing the distribution of the Caiuá and Bauru groups. (b) Detailed lithostratigraphic map of the northeastern Bauru Group deposits. (c) Study area near the Uberaba municipality with location of the Price 1, BR050, and Lafarge Quarry type-sections shown. Palaeocurrent mean vectors are 318° ($n = 11$) in BR050 and 340° ($n = 38$) in Price 1 sites. (d) Litho- and chronostratigraphic chart of the Bauru Basin. This figure was modified from Soares et al. (2018) [Correction added on 27 October 2020, after first online publication: Figure 1 has been replaced and a citation has been inserted in the caption.] [Colour figure can be viewed at [wileyonlinelibrary.com](https://onlinelibrary.wiley.com)]

Specifically, the uppermost unit of the Bauru Group (Marília Formation) records several contrasting depositional environments and lithological features throughout the basin, which historically has led to proposals for an intricate framework of incompatible stratigraphic units (e.g., Basilici, Fiorelli, & Dal' Bo, 2016; Soares et al., 2018).

The Marília Formation was first described by Almeida and Barbosa (1953) and the unit was later formalized by Soares et al. (1980) for the southeastern Bauru Group. The geographic coverage of this unit was later expanded towards the northeastern and northwestern parts of the Bauru Group, and Barcelos (1984) organized the formation into three members: the Echaporã Member in the southeastern and northwestern parts, and the Serra da Galga and Ponte Alta members restricted to the northeastern part of the Bauru Group. These members present a complex, interdigitated, and irregular contact with each other (Fernandes & Coimbra, 2000). As a result, the expansion of the Marília Formation northwards constructed an intricate

stratigraphic framework of members with unparalleled characteristics and with spatial coverage that is incompatible to the rank of 'member'. Recent studies have established a clear distinction among the lithologic, stratigraphic, palaeontological, palaeopedological, and palaeoenvironmental aspects of the northeastern deposits (Serra da Galga and Ponte Alta members) and those of their southeastern and northwestern counterparts (Echaporã Member; Basilici, Fiorelli, & Dal' Bo, 2016; Soares et al., 2018). For this reason, from here on, this work refers to the deposits of the Marília Formation exposed in the northeastern part of the Bauru Basin (traditionally subdivided in Serra da Galga and Ponte Alta members) as the Serra da Galga Formation. Consequently, the use of the term Marília Formation is here restricted to the southeastern and northwestern parts of the Bauru Basin, traditionally considered as the Echaporã Member.

In the southeastern and northwestern parts, the Marília Formation is mostly defined by very fine to fine-grained sandstones that

show varying degrees of carbonate cementation. Conglomeratic sandstone layers occur locally and constitute less than 5% of the total thickness of the succession. Thin and laterally restricted sandy-mudstone layers occur as lenses among sandstone layers and represent less than 2% of the total succession of the basin fill (Basilici, Dal'Bo, & Oliveira, 2016). The palaeontological content of the Marília Formation is dominated by fossils of theropod (abelisauroids) and sauropod (titanosaurs) dinosaurs, crocodyliforms, and ichnofossils (e.g., Bertini, Santucci, & Arruda-Campos, 2001; Iori & Arruda-Campos, 2016; Méndez, Novas, & Iori, 2014; Mineiro, Santucci, Da Rocha, De Andrade, & Nava, 2017; Santucci, 2013).

Conversely, the deposits of the Serra da Galga Formation are predominantly formed of medium- and coarse-grained sandstones, pebbly sandstones and conglomerates, plus groundwater-sourced calcrete beds, and in a minor amount fine-grained sandstones and mudstones (Soares et al., 2018). The lowermost contact of the Serra da Galga Formation is slightly erosive with deposits of the underlying Uberaba Formation. This unit is formed of very fine sandstones and silty mudstones showing clay-rich matrix and is subordinately interstratified with mudstone, claystone, conglomeratic sandstone, and conglomerates (Fernandes & Coimbra, 2000). The vertebrate palaeontological content of the Serra da Galga Formation is more diverse than that of the Marília Formation; fossils belong to several groups of fishes (e.g., siluriforms, lepisosteiforms, amiids, characiforms, perciforms, and dipnoans), anurans, podocnemid turtles, squamates (iguanians), mesoeucrocodylians (peirosaurids, itasuchids, 'advanced notosuchians'), theropods (e.g., abelisauroids, maniraptorans, aves) and titanosaur sauropods (e.g., Báez et al., 2012; Brito, Amaral, & Machado, 2006; Campos, Kellner, Bertini, & Santucci, 2005; Carvalho, Ribeiro, & Avilla, 2004; Kellner, Campos, & Trotta, 2005; Kellner, Figueiredo, Azevedo, & Campos, 2011; Martinelli et al., 2013; Martinelli & Teixeira, 2015; Novas, Carvalho, Ribeiro, & Méndez, 2008; Novas, Ribeiro, & Carvalho, 2005; Salgado & Carvalho, 2008). Moreover, the fossil record includes conchostracans, ostracodans, charophytans, molluscs (gastropods and bivalves; e.g. Carbonaro, Rohn, & Ghilardi, 2013; Dias-Brito et al., 2001; Ghilardi, D'Agosta, Alves, & Arruda-Campos, 2011) and ichnofossils (e.g., Francischini et al., 2016; Magalhães Ribeiro, 2002; Martinelli et al., 2019; Mineiro & Santucci, 2018; Paes Neto et al., 2018).

3 | METHODS

To propose a new lithostratigraphic classification for the northeast deposits of the upper Bauru Group, this work applied geological mapping, sedimentological, architectural, and palaeopedological characterization of the deposits. The geological mapping was conducted at a regional scale (1:25,000). A total of 80 outcrops were analysed through the mapping campaign covering an area of ca. 450 km² near the Uberaba municipality (Figure 1). Three main study sites were adopted as type-sections for the Serra da Galga Formation deposits: the Price 1 Geosite (19°43'26.89"S - 47°44'47.45"W; also known in the literature as 'Caieira Site' or

'Ponto 1 do Price'), the BR050 Geosite (19°35'32.39"S - 48°1'42.80"W; also known as BR050-km 153) and the Lafarge Quarry site (19°42'25.2"S - 47°40'34.7"W; Figure 1). Additionally, another 43 outcrops were used to better constrain the nature of the deposits. Sedimentological features were described through lithofacies and architectural element analysis. Twelve lithofacies were identified and described according to their genetic significance (Harms, Southard, & Walker, 1982; Miall, 2016; Walker, 2006) and based on their main sedimentological features: grain size, fabric, sorting, mineralogy, sedimentary structures, bounding surfaces, palaeocurrent indicators, bed thickness, geometry, and bioturbation. Palaeosols were identified among the deposits by the presence of destratification, patterns of vertical colour variation, root marks, nodules, bioturbation, and mottles (Catt, 1990; Retallack, 1988). Facies and palaeosol arrangements were assigned to common associations which themselves are present as the deposits of six architectural elements. The characterization of sedimentary architecture was based on the recognition of a set of hierarchical bounding-surface types delimiting facies associations, according to the method of Miall (2006). The lithostratigraphic classification of the studied unit was proposed according to the international code for stratigraphic nomenclature (Murphy & Salvador, 1999).

4 | THE SERRA DA GALGA FORMATION

The northeastern deposits of the upper Bauru Group occur in the study region over an area of ca. 450 km² centred on the municipality of Uberaba. At this location, the infill of the Bauru Basin comprises a maximum thickness of 260 m (Figure 2), rests directly over the exposed basalts of the Serra Geral Formation, and is composed of two main units, from the base to the top: (a) Uberaba Formation and (b) Serra da Galga Formation. The latter unit occurs as a laterally continuous horizontal layer with an average thickness of 100 m. The lower boundary is inferred to be slightly erosive with the underlying Uberaba Formation, as it reveals local topographic discontinuities in the lithostratigraphic map (palaeotopographic relief of 15–25 m). The upper boundary of the unit is marked by a geomorphologic surface that corresponds to a Cenozoic lateritic soil profile perceived as a flat topographic plateau with no observable topographic discontinuities evident from the regional geological mapping (Figure 2).

4.1 | Facies analysis

A total of eleven sedimentary facies and three main pedotypes were identified and described in the Serra da Galga Formation at three adopted type-sections (Figure 3). Facies are organized as belonging to channel and interchannel deposits. Channel deposits are composed of the following facies: (Cs) sandy conglomerate, (Sgtc) planar or trough cross-bedded pebbly sandstone, (Stc) trough cross-bedded sandstone, (Sl) large-scale lenticular cross-bedded sandstone, (Sgp) planar

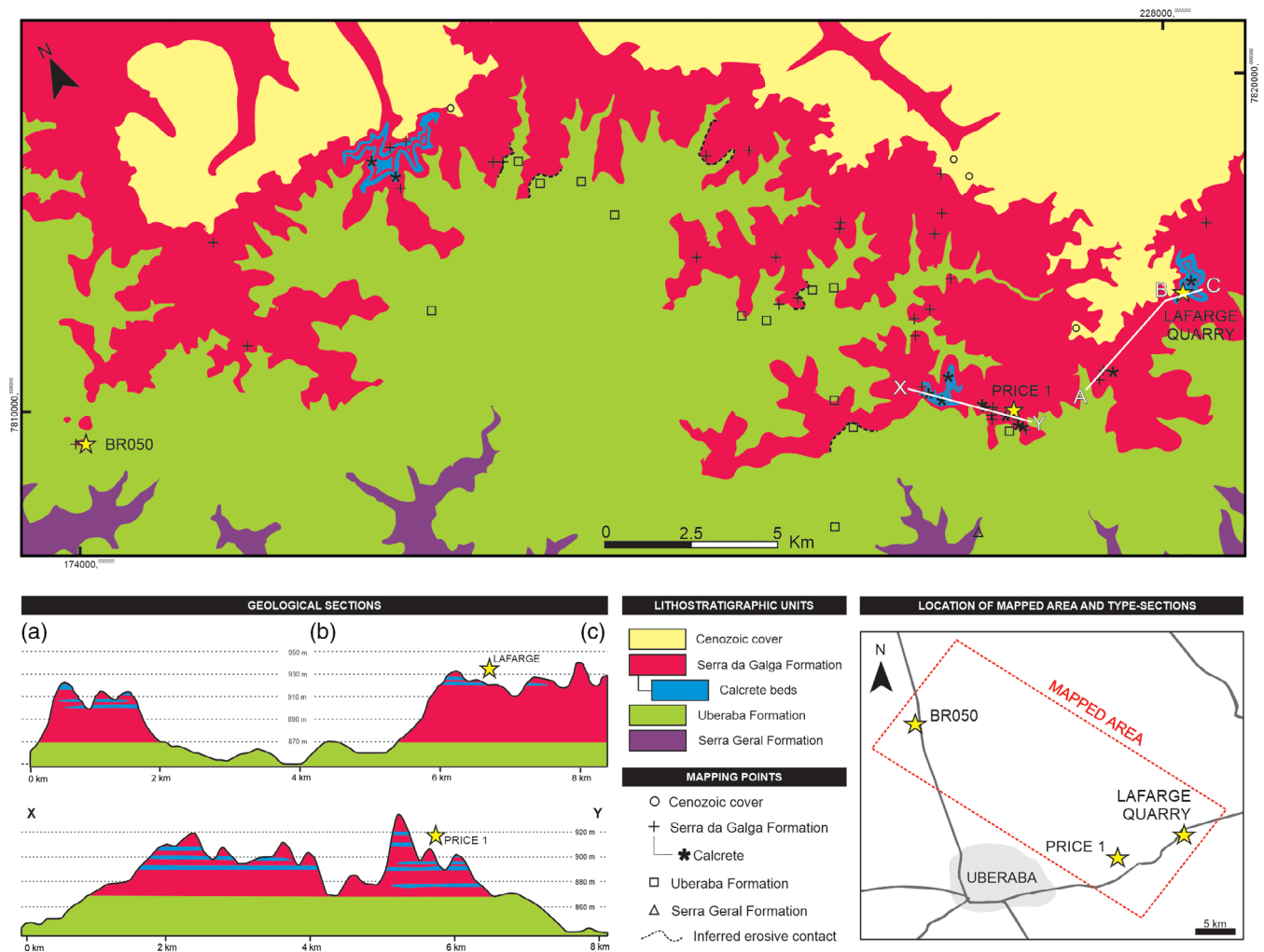


FIGURE 2 Lithostratigraphic map and geological sections of the study area [Colour figure can be viewed at wileyonlinelibrary.com]

cross-bedded conglomeratic sandstone, (Sfc) cross-laminated fine-grained sandstone, and (Sfp) planar-laminated fine-grained sandstone. Interchannel deposits are formed of the following facies: (Sf) fine sandstone, (Sm) muddy sandstone and (M) mudstone. Palaeosol profiles (P) and calcrete beds (C) occur interstratified among the deposits. Description and interpretation are provided below.

4.1.1 | Sandy conglomerate – Cs

Description: The sandy conglomerate (Figure 4f) is formed of tabular layers that extend laterally for more than 15 m and vertically up to 0.5 m. Bottom and top are outlined by horizontal erosive bounding surfaces. The sandy conglomerate shows matrix-supported organization where intraformational and extraformational clasts occur surrounded by coarse- to very coarse-grained lithoarenite matrix showing carbonate cementation. Overall, the conglomerate appears structureless, only locally marked by incipient normal grading.

Interpretation: The conglomerate is interpreted as product of hyperconcentrated flows formed by rapid deposition from bedload

and suspended load that inhibited any internal organization of the deposit (Costa, 1988). The flows were marked by transient pulses of turbulence resulting in deposits with incipient normal grading at places (Nemec & Steel, 1984).

4.1.2 | Planar and trough cross-bedded pebbly sandstone – Sg_{tc}

Description: The planar and trough cross-bedded pebbly sandstone (lithofacies Sg_{tc} – Figure 4a) is composed of planar and trough cross-stratified sets, 0.2–0.6 m thick and 0.2–3 m wide. Cross-strata are formed of alternating gravel and coarse- to medium-grained sandstone. The sets are organized in tabular sequences that extend laterally for more than 110 m and are up to 2 m thick. The bottom is erosive and the top exhibits gradual transition to the trough cross-bedded sandstone (lithofacies St_c). Extraformational clasts are rounded to well-rounded and polymictic (quartzite, gneiss, and chalcidony). Intraformational clasts are angular to sub-rounded (mudstone and pedogenic calcareous nodules). At the uppermost portion

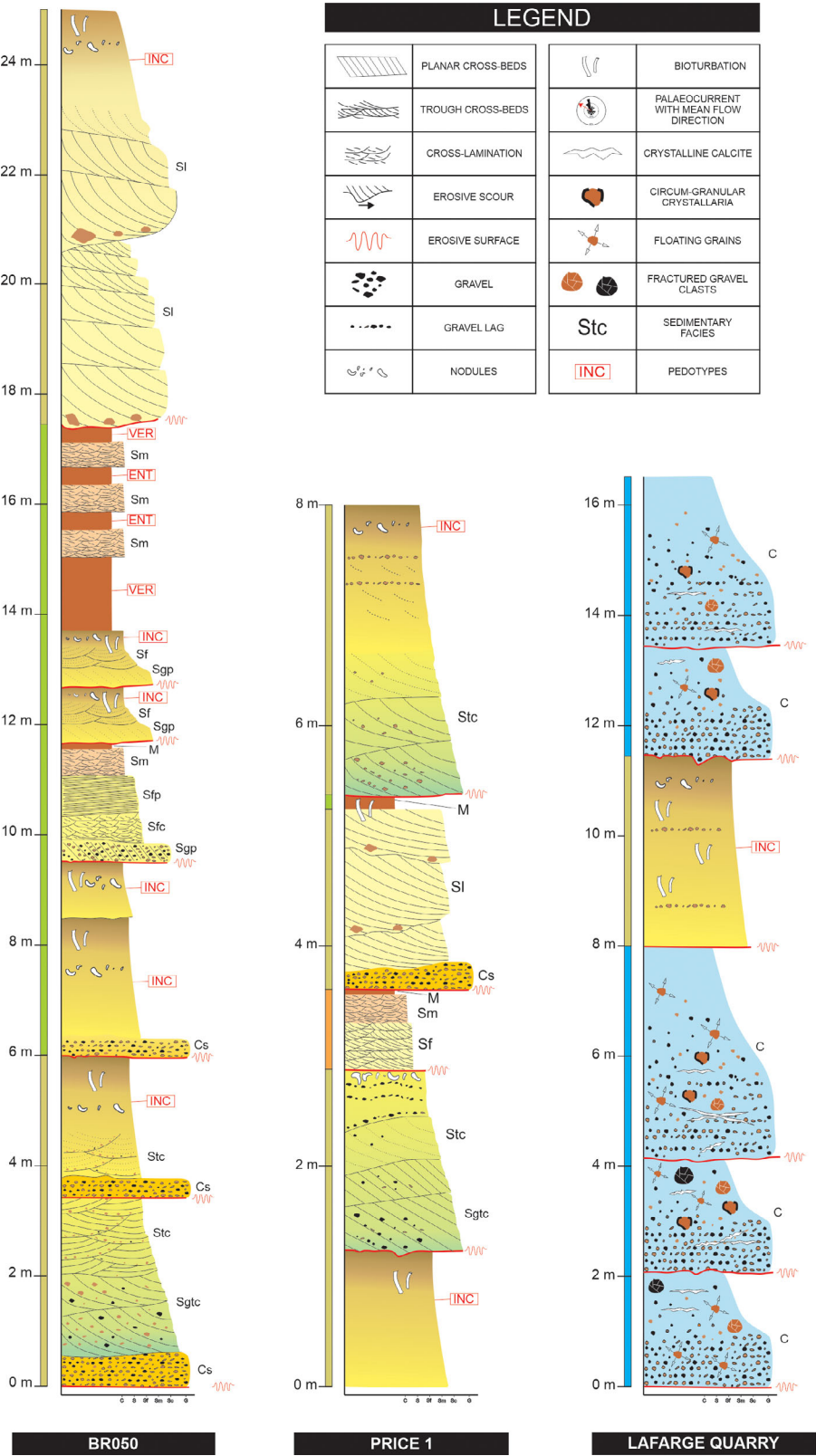


FIGURE 3 Stratigraphic sections of the Price 1, BR050, and Lafarge Quarry type-sections of the Serra da Galga Formation [Colour figure can be viewed at wileyonlinelibrary.com]

of the architectural element, trough cross-bedded sandstone (lithofacies Stc – Figure 4b) comprises trough cross-stratified sets, 0.1–0.4 m thick, organized in tabular layers that extend laterally for more than 110 m and vertically up to 2 m. The sandstone is

medium-grained and is characterized by granule and small pebble lags along foresets and at lower set boundaries. The top of the architectural element demonstrates palaeopedogenic alteration (palaeosol – lithofacies P).

Interpretation: This lithofacies is interpreted as a field of three-dimensional (3D) small transversal bars and/or dunes showing

superimposed smaller bedforms (planar and trough cross-bedded pebbly sandstone – lithofacies Sg_{tc}; Collinson & Mountney, 2019; Lunt,



FIGURE 4 Legend on next page.

Bridge, & Tye, 2004; Smith, 1972; Soares et al., 2018). The grain size alternation of the cross-bedding indicates the migration of superimposed bedforms with different grain sizes. The sandy cross-strata relates to the migration of smaller bedforms, whereas the gravel cross-strata is related to the migration of larger bedforms (Lunt et al., 2004).

4.1.3 | Trough cross-bedded sandstone – Stc

Description: The trough cross-bedded sandstone (Figure 4b) comprises trough cross-stratified sets, 0.1–0.4 m thick, organized in tabular layers that extend laterally for more than 110 m and vertically up to 2 m. The sandstone is medium-grained and is characterized by granules and small pebbles along foresets and at lower set boundaries. The top parts of units of this facies commonly demonstrates palaeopedogenic alteration (palaeosol – lithofacies P).

Interpretation: Deposition of this lithofacies relates to smaller 3D dunes (trough cross-bedded sandstone – lithofacies Stc) that overlay the previous dune field of 3D small transversal bar and/or dunes (lithofacies Sgtc). This facies is genetically related to the planar and trough cross-bedded pebbly sandstone (lithofacies Sgtc) and records a relative increase in sorting upwards during a progressive decrease in flow energy (Collinson & Mountney, 2019; Lunt et al., 2004; Smith, 1972; Soares et al., 2018).

4.1.4 | Large-scale lenticular cross-bedded sandstone – Sl

Description: Large-scale lenticular cross-bedded sandstone (Figure 4c) consists of lenticular cross-bedded sets, 10–15 m wide and up to 1.4 m thick. Cross-stratifications exhibit gentle to moderate dip angles (10–15°) with concave-up geometry, forming wedge-shape cross-strata that taper towards the toeset, which is tangential and long. These sets stack to form tabular layers that extend laterally for more than 110 m and are up to 2 m thick. The bottom surface is erosive and concave-up. The top is erosive with planar or slightly concave-up geometry. The sandstone is poorly to moderately sorted, coarse- to

medium-grained sublitharenite and can include numerous mudstone intraclasts.

Interpretation: This lithofacies is interpreted as large subaqueous dunes with low- to moderate-angle inclined foresets formed by near-supercritical, high-velocity currents controlled by a high concentration of suspended sediments (Jopling, 1965; Soares et al., 2018). The low-angle foresets and the abundant intraclasts indicate that flow velocity operated at the transition from dune to upper-stage plane-bed stability fields (Chakraborty & Bose, 1992).

4.1.5 | Planar cross-bedded conglomeratic sandstone – Sgp

Description: The planar cross-bedded conglomeratic sandstone (Figure 4d) occurs as lenticular layers ranging from 0.5 to 1 m in thickness. The sandstone lies above a slightly erosive, concave-up scoured base and is organized in tabular sets (0.15–0.40 m thick) that are planar cross-stratified. Foresets dip angles vary from 20° to 25°. Sets show a fining-upward trend in which the base is composed of conglomeratic sandstone, grading to medium-grained sandstone, to fine-grained sandstone at the top. The gravels are primarily formed of subangular to angular mudstone and carbonate cemented sandstone intraclasts (granules to pebbles) and secondarily of subrounded to rounded extraformational clasts. The matrix is composed of fine-grained sand.

Interpretation: The scoured base indicates probable erosion from poorly channelized floods, followed by deposition from small-scale two-dimensional (2D) dunes under shallow-water conditions (Miall, 2006).

4.1.6 | Cross-laminated fine sandstone – Sfc

Description: The cross-laminated fine sandstone (Figure 4e) forms tabular layers that are laterally continuous and range in thickness up to 0.3 m. The sandstone is organized in lenticular sets (10–30 mm thick) with low-angle foresets of tabular cross-stratifications. Grains are subrounded to rounded and vary from very fine sand to silt.

FIGURE 4 Sedimentary facies of the Serra da Galga Formation. (a) Trough cross-bedded pebbly sandstone (lithofacies Sgtc) showing cross-strata of alternating gravel (G) and coarse- to medium-grained sandstone (SG). (b) Trough cross-bedded sandstone (lithofacies Stc) with granules and small pebbles associated with foreset and set boundaries. (c) Large-scale lenticular cross-bedded sandstone (lithofacies Sl) with concave-up erosive base marked by abundant mudstone intraclasts. Cross-strata show gentle dip angles (10–15°). (d) Planar cross-bedded conglomeratic sandstone (lithofacies Sgp) with foreset dip angles that vary from 20° to 25°. (e) Cross-laminated fine sandstone (lithofacies Sfc) formed of lenticular sets (10–30 mm thick) with low-angle foresets. (f) Sandy conglomerate (lithofacies Cs) showing massive sets and matrix-supported organization of clasts. (g) Planar-laminated fine sandstone (lithofacies Sfp) organized in laminae couplets showing a clear bimodal grain-size distribution between fine sand and silt. Laminae thickness is a few grain diameters. (h) Fine-grained sandstone (lithofacies Sf) formed of sets of small-scale trough cross-strata with foreset dip angles between 15 and 20°. (i) Muddy sandstone (lithofacies Sm) organized in lenticular sets with cross-laminations outlined by mud drapes. The structureless mudstone (lithofacies M) occurs at the top of the muddy sandstone (lithofacies Sm). Coin diameter in [A,D,F,G] is 30 mm. Coin diameter in [E,I] is 20 mm. Hammer length [B] is 28 cm [Colour figure can be viewed at wileyonlinelibrary.com]

Interpretation: This lithofacies is the product of deposition from subaqueous ripples indicating low-energy flow conditions (Jopling & Walker, 1968).

4.1.7 | Planar-laminated fine sandstone – Sfp

Description: This lithofacies (Figure 4g) forms laterally continuous layers up to 0.6 m thick. The bottom surface is erosive with the cross-laminated fine-grained sandstone (lithofacies Sfc). Sediments vary from very fine sand to silt; grains are subrounded to rounded. The sandstone is organized in couplets of laminae; each lamina is a few grain thick, showing a clear bimodal grain-size distribution where a lamina of fine sand alternates with a lamina of very fine sand and silt.

Interpretation: The presence of flat-lying planar-laminations indicate upper-regime plane-bed conditions, possibly associated with a decrease in the cross-sectional area of floods in an unconfined flow (Paola, Wiele, & Reinhart, 1989).

4.1.8 | Fine-grained sandstone – Sf

Description: The fine-grained sandstone (Figure 4h) is composed of tabular layers that are no more than 25 m wide ca. 0.5 m thick. It is organized in sets (0.1–0.2 m thick) that are lenticular in shape. The sets are composed of small trough cross-stratifications with dip angles from 15° to 20°. Foresets are marked by mud drapes. Set bounding surfaces are outlined and defined by mudstone laminae.

Interpretation: The fine-grained sandstone indicates initial overbank sedimentation from small 3D dunes with sinuous crests deposited under shallow-water conditions. The presence of mud laminae indicate episodes of stagnant water or oscillations of the flow energy during dune migration during probable falling water stages (Coronel, Isla, Veiga, Mountney, & Colomera, 2020; Miall, 2006).

4.1.9 | Muddy sandstone – Sm

Description: The muddy sandstone (Figure 4i) occurs as tabular layers that extend laterally for no more than 25 m with thickness of ca. 0.3 m. The sandstone is organized in lenticular sets with cross-laminations (1–30 mm thick) that are outlined by mud drapes.

Interpretation: The muddy sandstone is formed by mutually erosive type-A ripples formed under shallow-water conditions (Jopling & Walker, 1968). The occurrence of mud drapes indicates low energy alternations between episodes of overbank floods and stagnant waters (Banham & Mountney, 2014).

4.1.10 | Mudstone – M

Description: The mudstone (lithofacies M – Figure 4i) forms tabular layers that extend laterally to no more than 5 m and are ca. 0.05 m

thick. The lithofacies is structureless and shows local levels of bioturbation consisting of millimetre-scale tubules filled with facies Sm.

Interpretation: The mudstone indicates sedimentation operated solely by settling of mud (mudstone – lithofacies M) under stagnant water conditions (Miall, 2006). The presence of bioturbation indicates a marked decrease of the environmental energy (Hubert & Hyde, 1982).

4.1.11 | Palaeosols – P

Description: Three main pedotypes are identified in the Serra da Galga Formation: (a) Entisols, (b) Inceptisols, and (c) Vertisols.

The Entisols are formed of compound profiles of A-C horizons that range in thickness from 0.2 to 0.4 m and ultimately form sequences that reach up to 2.5 m vertically (Figure 5). This pedotype develops over fine-grained deposits (lithofacies Sf, Sm, and M). The A horizon, 0.1–0.4 m thick, displays a pink colour (7.5YR 7/3), is bioturbated (Figure 6a) and has mud-filled root casts (Figure 6b) that locally cross the A-C boundary. The C horizon, 0.2–0.4 m thick, is white to light pink in colour (7.5YR 8/0, 8/2) and is identified by the presence of relic clay laminae interspersed with lenticular sets of cross-laminated fine sandstone (lithofacies Sf, Sm, M). Rare bioturbation is also observed in this horizon. The A-C boundary is diffuse, whereas the A horizons are commonly truncated by erosive surfaces.

The Inceptisols form complete sequences of A-Bw-Bk-Ck (or C) horizons in profiles that are 1–2 m thick (Figure 5). This pedotype is developed over sandstones (lithofacies Sgtc, Stc, Sgp, Sfc, and Sfp). The A horizon is seldom preserved and is marked by whitish-pink colour (7.5YR 7/3). When present, it reaches no more than 0.4 m in thickness. The horizon shows drab haloed root traces (Figure 6c) and locally reveals coalescent bioturbation. The cambic (Bw) horizon is 0.3–1.2 m thick, shows slightly higher chroma value (pink – 7.5YR 7/3) and is further distinguished by more intense bioturbation and weak micritic carbonate cementation. The calcic (Bk) horizon can occur where associated with intense micritic to microsparitic carbonate cementation (Figure 6d) that impregnates the palaeosol matrix and highlights bioturbation. The C horizon, 0.4–1.2 m thick, is identified by the presence of relic sedimentary structures (e.g., planar- and cross-laminated fine sandstone – Sfp, Sfc; trough and planar cross-bedded sandstone – Sgp, Sgtc, Stc; conglomerate – Cs). Moderate to strong carbonate cementation is present in calcic (Ck) horizons.

The Vertisols typically display a sequence of horizons Assk-Bssk, up to 0.7 m thick (Figure 5). This pedotype appears associated with fine-grained deposits (lithofacies Sf, Sm, and M). The Assk horizon, 0.1–0.3 m thick, is light pink in colour (7.5YR 8/2) and reveal gilgai microrelief that are formed of an undulose surface composed of microhighs, with angular blocky peds (2–20 mm in diameter), and microlows that form lenticular peds (up to 40 mm thick and 0.3 m wide; Figure 6e). Both angular blocky and lenticular peds are coated by red-coloured clay skins (*argillan*). Rhizocretions (Figure 6e) occur in this horizon and are laterally coalescent, locally forming clusters that are up to 0.5 m wide. The Bssk horizon, 0.1–0.4 m thick, is slightly

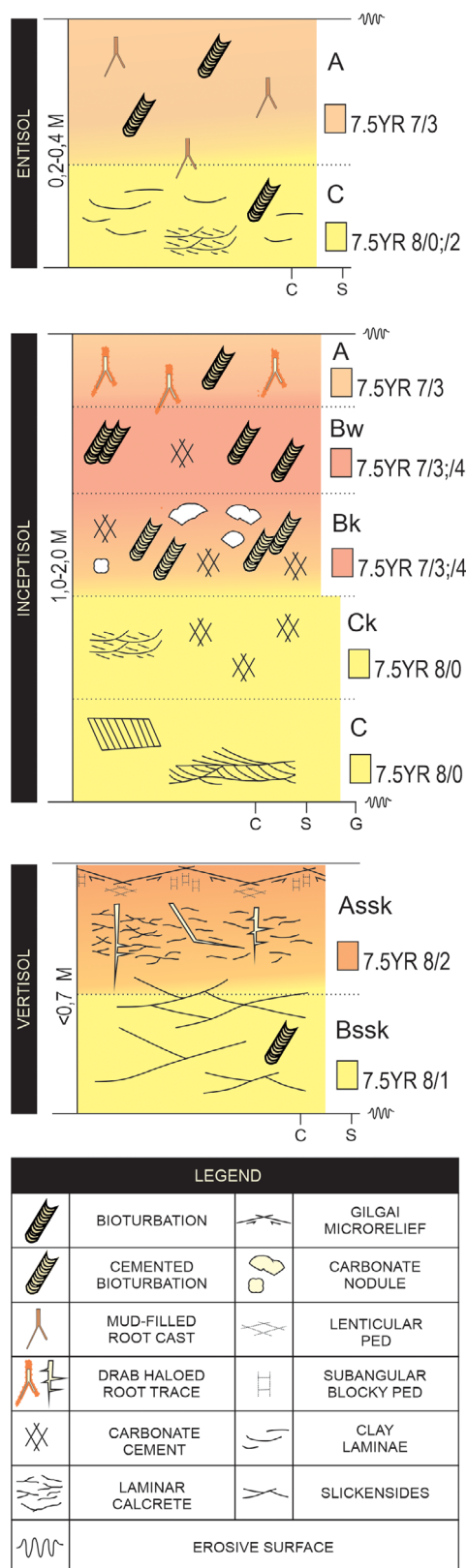


FIGURE 5 Pedotype profiles of the Serra da Galga Formation organized as Entisol, Inceptisol, and Vertisol profiles [Colour figure can be viewed at wileyonlinelibrary.com]

lighter in colour and shows lower chroma (light pink – 7.5YR 8/1). It also contains angular blocky and lenticular peds. Rhizocretions are less common, whereas bioturbation is common. The Assk-Bssk boundary is diffuse, whereas the A horizon is bounded at the top by undulated gilgai microrelief.

Interpretation: Palaeosols (lithofacies P) that occur interbedded with the interchannel deposits and channel fills are robust indicators of long pauses in sedimentation that are associated with topographic surface stability to the order of several hundred or possibly thousands of years (Kraus, 1999). Inceptisols appear at the top of large-scale channel fills (types 1 and 2) and also atop the small-scale poorly channelized crevasse channel fills (type 3). The thin and low chroma A horizon can be associated with an ochric epipedon, which overlies horizons with higher chroma (Bw) or cemented by calcium carbonate (Bk). These characteristics permit association of this pedotype to Inceptisols (Soil Survey Staff, 2014). Their occurrence within channel deposits may indicate a brief interavulsion period associated with large-scale channels (Kraus, 1999). Entisols are restricted to interchannel deposits and are classified according to their typical sequence of A-C horizons (Soil Survey Staff, 2014). The stratigraphic framework of Entisols interbedded with interchannel deposits can be associated with overbank areas of higher sedimentation rate that are mostly situated near the active channels (Kraus, 1999). Vertisols are identified by their higher clay content and the presence of gilgai microrelief, slickensides, and subangular to lenticular blocky peds (Soil Survey Staff, 2014). They occur restricted to interchannel deposits and indicate repeated wet-dry episodes typical of distal lowlands where the local slope does not exceed 3% (Young, 1976) to 5% (Mohr, Van Baren, & Van Schuylenborgh, 1972).

4.1.12 | Calcrete – C

Description: The calcretized conglomeratic sandstone shows fining-upward trends (Figure 7b). At the base, the calcrete is formed of oligomictic, matrix-supported sandy conglomerate composed of granules and pebbles of subangular to subrounded lithic fragments, locally showing ventifacts (Figure 7b). The sandstone is a lithoarenite constituted of medium to coarse sand grains. Calcrete bodies are predominantly marked by alpha-type carbonate microstructures (sensu Wright, 1990). Their margins show lower grade of calcium carbonate cementation and are composed of a dense and continuous micritic groundmass characterized by sparse floating grains of lithoarenite (Figure 7c). These features persist through the entire calcrete layer. At the central portion of the calcretized layer, the carbonate crystals increase in size in the groundmass and range from micrite to spar (Figure 7d). In places, the distribution of carbonate minerals occurs in patches of different crystal sizes, forming a mottled fabric. Additionally, calcite-filled cracks (crystallaria, sensu Wright & Tucker, 1991) are present into the centre of calcrete beds. Cracks are common and predominantly interconnected and subhorizontal (crossing at angles of

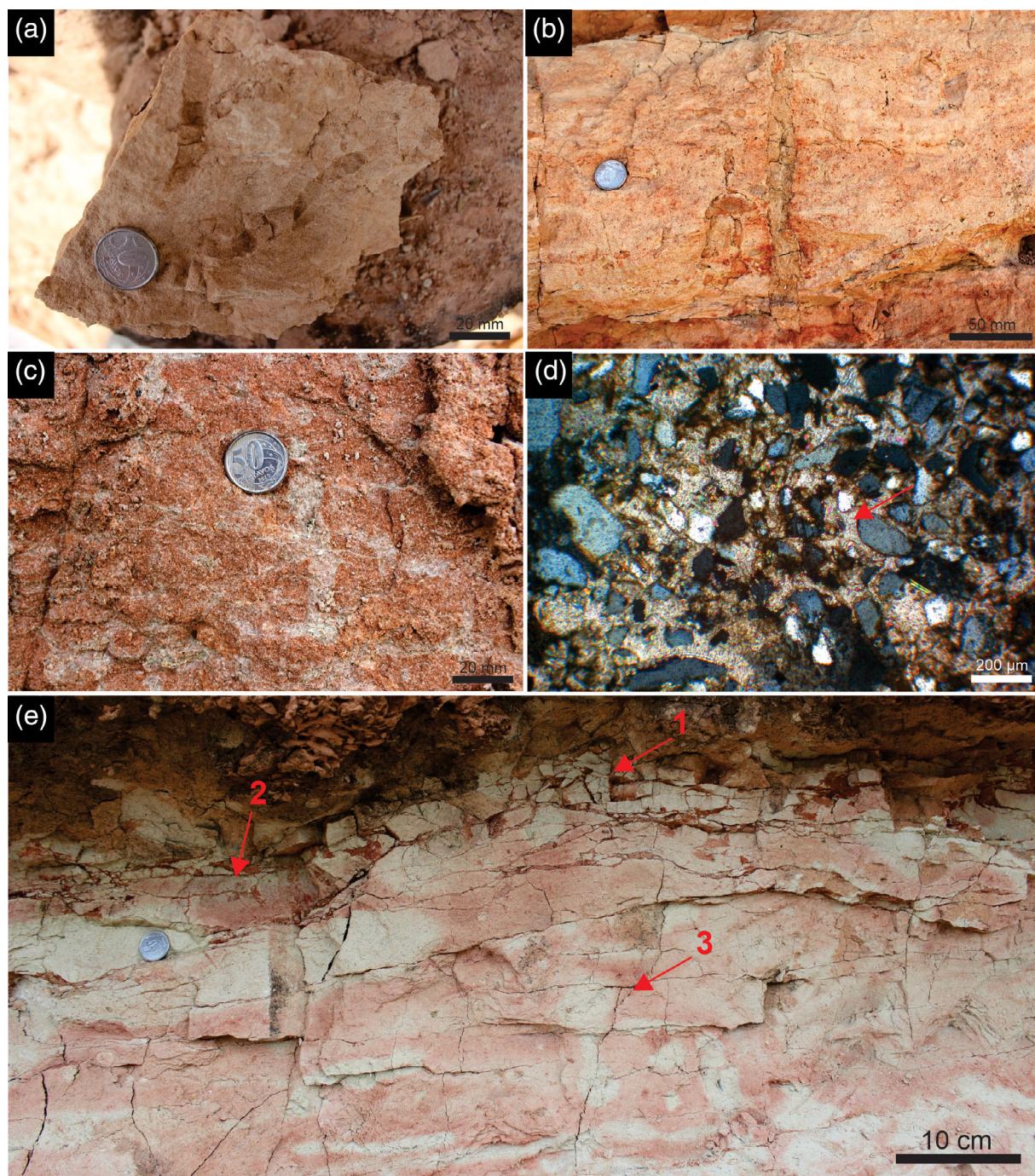


FIGURE 6 Pedofeatures observed in palaeosols of the Serra da Galga Formation. (a) Bioturbation structures and (b) vertical mud-filled root cast in Entisol profiles. (c) Drab haloed root traces observed in the A horizon of an Inceptisol profile. (d) Impregnative calcite cement (arrow) in the micromass of a Ck horizon of an Inceptisol profile. (e) Vertisol profile showing gilgai microrelief composed of subangular blocky peds in the microhighs (1) and lenticular peds in the microlows (2). Clusters of rhizcretions revealed by haloes of Fe reduction (3) [Correction added on 27 October 2020, after first online publication: Figure 6a and its corresponding legend has been updated.] [Colour figure can be viewed at wileyonlinelibrary.com]

60°–120°); locally, channels (up to 50 mm thick) and brecciated fabric with infillings of calcite with irregular to well-formed crystal faces are observed (Figure 7e). Extraformational granules and pebbles of the parent material commonly reveal circum-granular crystallaria features with microsparitic to sparitic calcite infilling (Figure 7c,d). Locally, gravel clasts show intense fracturing (up to 2 mm thick fractures) filled

by dense and micritic groundmass with floating-grain fabric (Figure 7c,f).

Interpretation: Calcrete beds are related to post-depositional phreatic cementation of carbonate-rich groundwater in the capillary fringe zone of shallow-water aquifers (e.g., 1–3 m deep; Mann & Horwitz, 1979; Netterberg, 1969; Pimentel, Wright, &

Azevedo, 1996; Wright & Tucker, 1991). The abundance of a suite of alpha-type carbonate microfabrics in the calcrete beds indicates abi-
otic genesis driven by near-surface processes (Wright, 1990) of

displacive and replacive carbonate growth enforced by arid to semi-
arid climates through moisture infiltration, carbonate dissolution,
evaporation, and evapotranspiration (Wright & Tucker, 1991).



FIGURE 7 Legend on next page.

Because groundwater calcretes are formed below the biological activity zone, beta-type calcretes are not usually observed in these types of calcretes. Instead, groundwater calcretes are typically micritic and frequently composed of crystalline mosaics of variable sizes, floating grains texture and desiccation cracks (Wright & Tucker, 1991), as similarly observed in the interstratified beds in the Serra da Galga Formation. The abundance of calcite-filled cracks (crystallaria) of various geometries and dimensions indicates intense desiccation and expansive growth, creating large pores where evaporation and degassing effects promote rapid carbonate precipitation (Wright & Tucker, 1991). Floating grains and grain expansion reflect the displacive carbonate growth that is typical of groundwater calcretes. At first stage, calcite cementation forms rapidly at grain contacts and intragranular fractures after supersaturation of pore fluids in the vadose zone, forcing a stress in grain contacts and ultimately fracturing them and allowing calcite cement into the newly formed fractures (e.g., fractured gravels). At a second stage, in the phreatic zone, cement growth would not be limited to grain edges. Instead, calcite nucleation occupied the entire pore spaces, causing the dispersal of grains, finally culminating in the complete cementation of the sandstone, forming the densely micritic cement with floating grains (Buczynski & Chafetz, 1987).

4.2 | Architectural elements

Sedimentary facies and palaeosols were further assigned to architectural elements. Sedimentological and stratigraphic analysis at the study sites (Figures 8 and 9) revealed six architectural element types: (a) type 1 channel fill, (b) type 2 channel fill, (c) type 3 channel fill, (d) interchannel, (e) palaeosol, and (f) calcrete beds. The description and interpretation of these architectural elements are synthesized in Table 1.

4.2.1 | Type 1 channel fill

Description: The type 1 channel fills are the most abundant architectural elements of the succession and they appear highly amalgamated in the stratigraphic succession. They comprise horizontal layers that persist laterally for more than 100 m, varying from 2 to 7 m in thickness (Figure 8). The bottom and top bounding surfaces are erosive. The channel body is formed of a fining-upward succession of facies that show an increase in sorting upward: (a) planar and trough

cross-bedded pebbly sandstone (lithofacies Sg_{tc}) and (b) trough cross-bedded sandstone (lithofacies St_c).

Interpretation: The type 1 channel fills correspond to large channels (2.0–7.0 m deep) in which deposition was controlled by flows showing progressive decrease in energy, depth, and capacity over time. The fining-upward succession of lithofacies Sg_{tc} and St_c indicate waning flow, whereby channels were initially filled with a field of 3D small transverse bars and/or dunes with superimposed smaller bedforms (lithofacies Sg_{tc}), undergoing steady decrease in flow energy associated with the formation of smaller 3D dunes (lithofacies St_c) that progressively overlaid the previous bars and dune fields. Soares et al. (2018) have interpreted the type 1 channel fills as related to flows characterized by particularly steady conditions, fostered by periods of higher humidity in which groundwater supply to the channels was possible.

4.2.2 | Type 2 channel fill

Description: The type 2 channel fills are formed of horizontal layers that extend laterally for more than 100 m and vary in thickness from 1.5 to 8 m. These channels occur highly amalgamated in the stratigraphic interval (Figure 8). The bottom and top bounding surfaces are erosional. The channel body is composed of two main lithofacies, from the base to the top: (a) sandy conglomerate (lithofacies Cs) and (b) large-scale lenticular cross-bedded sandstone (lithofacies Sl).

Interpretation: The type 2 channel fills are related to large channels (1.5–8.0 m deep) in which deposition was governed by high-energy, fast-changing flows. Channel filling was initiated with the entrance of hyperconcentrated flows carrying abundant mudstone intraclasts, likely converging from the interchannel area into the channels (lithofacies Cs). Subsequently, channels were filled with a field of large transitional subaqueous dunes at flow speed near critical conditions, carrying large quantities of suspended load (lithofacies Sl). Soares et al. (2018) related the type 2 channel fills to drier periods, during which floods might have been associated with non-steady flow due to lack of connectivity with groundwater supply.

4.2.3 | Type 3 channel fill

Description: The type 3 channel fills appear interbedded with interchannel deposits. These channels form flattened bodies that extend laterally for 100 m and show thickness ranging from 1.0 to 1.5 m

FIGURE 7 Stratigraphic and lithological features of the Lafarge Quarry type-section. (a) Beds of calcretized conglomeratic sandstone bodies up to 8 m thick. (b) Slab of intensely calcretized conglomeratic sandstone showing normal grading, fractured pebbles and crystalline calcite venules. (c) Photomicrography of mildly calcretized pebbly sandstone showing sparse micritic groundmass characterized by floating grains, locally displaying micritic circum-granular crystallaria [1] and intragranular cracks filled with micritic calcite [2]. (d) Photomicrography of intensely calcretized pebbly sandstone showing sparse floating grains in a micritic to sparitic groundmass. Arrows indicate sparitic circum-granular crystallaria displaying growth of calcite crystals perpendicular to the grain margin. (e) Interconnected calcite-filled cracks forming brecciated fabric. (f) Photomicrography of intensely calcretized quartz grain displaying micritic to sparitic calcite infilling [1] and remnant of circum-granular crystallaria [2] [Colour figure can be viewed at wileyonlinelibrary.com]

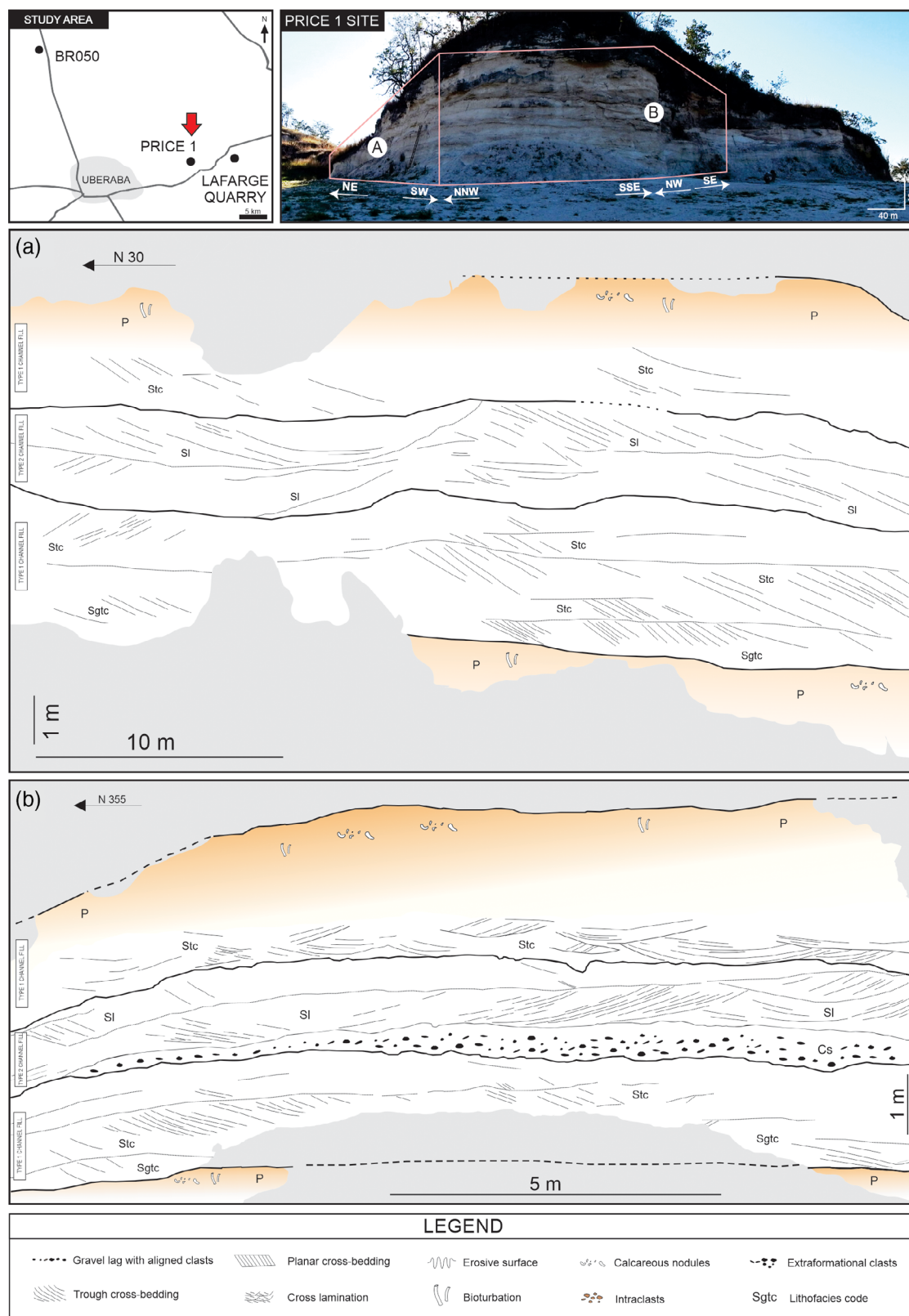


FIGURE 8 Stratigraphic framework of the Price 1 type-section showing architectural sketches in two directions: (a) approximately parallel to palaeocurrent direction and (b) approximately perpendicular to palaeoflow [Colour figure can be viewed at wileyonlinelibrary.com]

(Figure 9a). The bottom bounding surface is erosive and slightly concave-up while the top is flat. The type 3 channel fills display a clear

fining-upward sequence of facies, from base to top: (a) planar cross-bedded conglomeratic sandstone (lithofacies Sgp), (b) cross-laminated



FIGURE 9 Stratigraphic framework of the BR050 type-section showing two architectural sketches. (a) Crevasse channel fill formed of a fining-upward sequence of planar cross-bedded conglomeratic sandstone (lithofacies Sgp), cross-laminated fine-grained sandstone (lithofacies Sfc), and planar-laminated fine-grained sandstone (lithofacies Sfp). (b) Interchannel deposits characterized by alternations between lithofacies Sf and Sm [Colour figure can be viewed at wileyonlinelibrary.com]

fine-grained sandstone (lithofacies Sfc), and (c) planar-laminated fine-grained sandstone (lithofacies Sfp). These bodies appear in the stratigraphic record of the interchannel areas as poorly channelized structures consisting of a central, more deeply scoured base, which passes laterally into a shallow, slightly erosive margin (Figure 9a). This geometric arrangement is related to lateral variations in the distribution

of facies. The central scoured base is filled with conglomeratic sandstone, whereas, in portions towards their marginal terminations, the channel fills consist of fine-grained sandstones (Figure 9a).

Interpretation: The type 3 channel fills correspond to small-scale (1.0–1.5 m deep) channelized features that resemble isolated crevasse channels that occupy non-channelized portions of the overbank

TABLE 1 Description and interpretation of the architectural elements of the Serra da Galga Formation [Colour table can be viewed at wileyonlinelibrary.com]

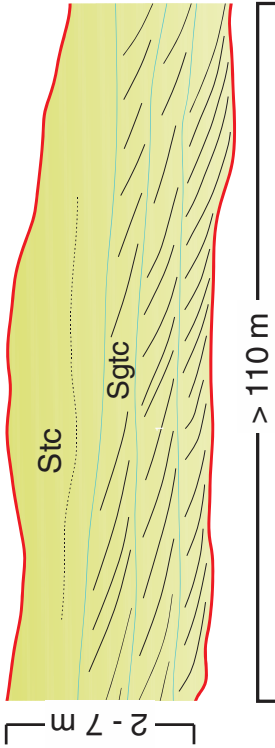
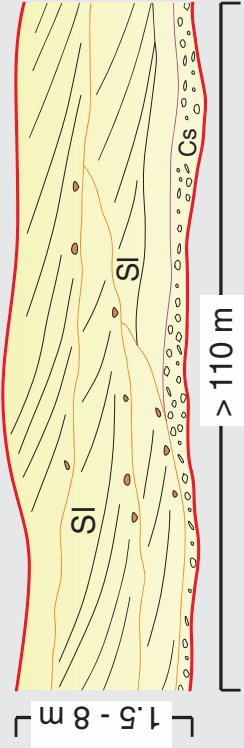
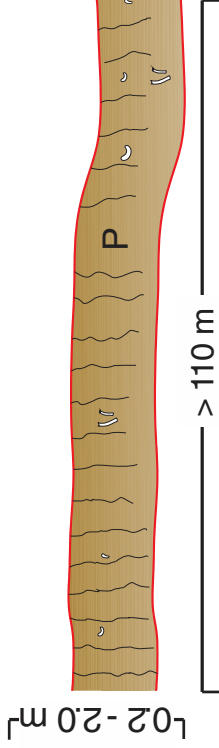
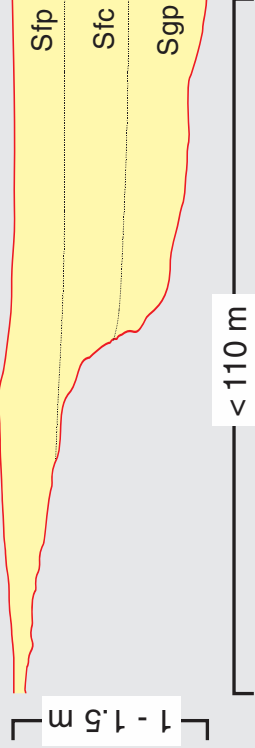
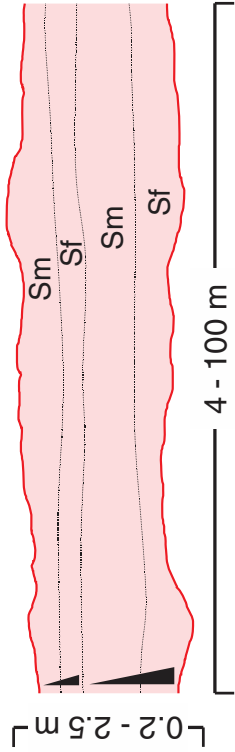
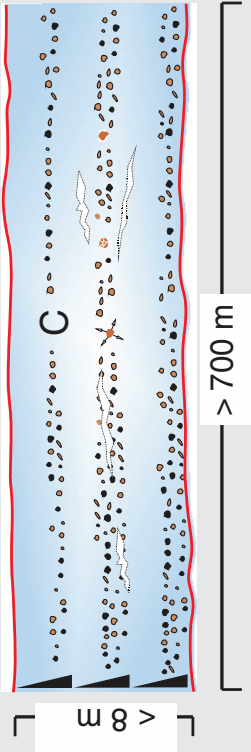
Architectural element	Sketch	Description	Interpretation
Type 1 channel fill		Horizontal layers that extend laterally for more than 100 m and vary in thickness from 1.5 to 8 m. The bottom and top bounding surfaces are erosional. The channel body is composed of two main lithofacies, from the base to the top: Cs - Sl	Large channels in which deposition was governed by high-energy, fast-changing flows. These channels are linked with dryer periods (Chakraborty & Bose, 1992; Costa, 1988; Jopling, 1965; Nemec & Steel, 1984; Soares et al., 2018).
Type 2 channel fill		Horizontal layers that persist laterally for more than 100 m varying from 2 to 7 m in thickness. The bottom and top bounding surfaces are erosive. The channel body is formed of fining-up sequences of facies that show increase in sorting upward: Sgfc - Stc.	Large channels controlled by flows showing progressive temporal decrease in energy, depth, and capacity. These channels are associated with more humid periods (Collinson & Moutney, 2019; Lunt et al., 2004; Miall, 2006; Soares et al., 2018).
Palaeosol		Tabular layers that extend laterally for more than 110 m and range from 0.2 to 2.0 m thick. They are organized in three pedotypes with the following complete sequence of horizons: Entisols [A-C], Inceptisols [A-Bw-Bk-Ck(or C)], and Vertisols [Assk-Bssk].	This architectural element is interpreted as palaeosols, which indicate long pauses on sedimentation associated with topographic surface stability for several hundred or possibly thousands of years (Retallack, 1988).
Type 3 channel fill		Sheet-like bodies that extend laterally for 100 m and show thickness that vary from 1.0 to 1.5 m. The bottom bounding surface is erosive and slightly concave-up while the top is flat and erosive. Sheet channels demonstrate a clear fining-upward sequence of facies, from the base to the top: Sgp - Sfc - Sfp.	Small-scale crevasse channels in the interchannel environment that are filled during floods from nearby feeder channels. Deposition is marked by 2D dunes, ripples, and less frequently upper-plane planar laminations (Burns, Mountney, Hodgson, & Colombero, 2017; Jopling & Walker, 1968; Miall, 2006; Paola et al., 1989).

TABLE 1 (Continued)

Architectural element	Sketch	Description	Interpretation
Interchannel		Tabular layers limited by erosive surfaces that appear interbedded with channel elements. These deposits demonstrated a highly variable lateral extension (4–100 m) and thickness (0.2–2.5 m) due to frequent erosion with surrounding channelized deposits. They are constituted of a clear fining-up sequence of facies, from the base to the top: Sf – Sm – M.	Interchannel deposits marked by deposition of unconfined 3D dunes, type-A ripples and mud (Hubert & Hyde, 1982; Jopling & Walker, 1968; Miall, 2006).
Calcrete bed		Laterally discontinuous layers of intensely calcretized sandstone, up to 15 m thick and 700 m in lateral extension. Lower and upper transitions are diffuse. Internally, the calcrete beds are formed of fining-up sequences of conglomeratic sandstone that are highly cemented by calcium carbonate, showing alpha microfabrics composed of circum-granular crystallaria, crystalline calcite cracks, mottles, floating grains, and fractured gravels.	Calcrete beds are associated with groundwater cementation during conditions of shallow water aquifers (Mann & Horwitz, 1979; Nettekberg, 1969). Cementation imprinted more effectively on coarse-grained deposits in the proximal and medial parts of the distributive fluvial system deposits (Nash & Smith, 1998; Tandon & Narayan, 1981).

environment. The lenticular geometry of these elements, their average thickness (1.0–1.5 m), as well as their interstratified association to overbank deposits, resemble crevasse channels described by Burns et al. (2017). The sand-prone infilling indicates a close proximity to the parent feeder channel (Burns et al., 2017; Nichols & Fisher, 2007). When the parent channel is subject to flooding, the peripheral crevasse channels that irradiate from the flood-breach are invaded by the flood waters. At each flood episode, a waning flow depositional history is recorded. Sedimentation begins at the central scoured section of the depression with deposition of 2D dunes (lithofacies Sgp) changing upward and laterally to ripples (lithofacies Sfc), marking a temporal and spatial decrease in flow energy. The channel is filled with sand until it becomes levelled with the floodplain, forcing the flood waters to spill onto the overbank and become unconfined (Nichols & Fisher, 2007). This process of channel overflow causes a decrease in the cross-sectional area of the floods; in order to maintain the passage of the same amount of volume of fluid into a narrower area, flows are forced to accelerate (Bernoulli effect). As a result, the top of the crevasse channels are marked by upper plane beds deposited from high-velocity overflows (lithofacies Sfp; Collinson & Mountney, 2019).

4.2.4 | Interchannel

Description: The interchannel architectural element takes the form of tabular layers enclosing type 3 channel fill elements. The interchannel deposits exhibit highly variable lateral extent (4–100 m) and thickness (0.2–2.5 m), due to their erosive contact with channelized deposits (Figure 9). Interchannel deposits form fining-upward facies sequences, from the base to the top: (a) fine-grained sandstone (lithofacies Sf), (b) muddy sandstone (lithofacies Sm), and (c) mudstone (lithofacies M).

Interpretation: The interchannel deposits are marked by the interbedding of deposits of unconfined floods and poorly channelized flows and palaeosols. Sedimentation in the interchannel areas occurs through alternations between flood episodes coming from the active channels (cf. Coronel et al., 2020). Small 3D dunes (lithofacies Sf) showing sinuous crests signify the commencement of deposition from floods. Mud-drape interlaminae are interpreted as developing in stagnant water ponds. Type-A ripples (lithofacies Sm) indicate later decline in flow energy, culminating in the termination of bedload input and overall energy decrease in the local sub-environment, together with the formation of stagnant water remnants within which deposition is exclusively by settling of mud particles (lithofacies M; Hubert & Hyde, 1982; Jopling & Walker, 1968; Miall, 2006).

4.2.5 | Palaeosols

Description: Palaeosol profiles (lithofacies P – Figure 5) are ubiquitous features that occur interbedded among deposits of the Serra da Galga Formation. They generally constitute tabular horizons that exceed 100 m laterally and range from 0.2 to 2.0 m in thickness. Three main

pedotypes are observed in the stratigraphic record of the Serra da Galga Formation: Entisols, Inceptisols, and Vertisols.

Interpretation: These pedotypes reveal an overall low degree of maturity. Vertisols and Entisols occupy the interchannel areas whereas Inceptisols, showing a slightly higher grade of development, occur in the large-scale channel belts and locally at the top of type 3 channel fills isolated in interchannel deposits. Normally, more immature soils are expected to be encountered near active channels, whereas more mature soils would be developed on overbank areas that are more distal to relative to sediment inputs. However, the opposite pattern is observed in this unit. A possible cause for this pattern might be the development of elevated channel ridges, whereby topographically elevated (i.e., superelevated) channel-belt areas become stabilized surfaces for longer periods after channel avulsion (see Soares et al., 2018 for further detail on the avulsion mechanism), thereby permitting the development of Inceptisols, whereas interchannel areas become preferential sites for deposition and erosion. The overall low degree of maturity of the palaeosols might be associated with high sedimentation rates, as well as with high avulsion frequency. Nevertheless, the factors controlling the distribution of palaeosols in the Serra da Galga Formation are complex and remain partly unresolved.

4.2.6 | Calcrete beds

Description: Beds of calcretized pebbly sandstone (Lithofacies Sg_{tc} – Figure 7) occur along the Serra da Galga Formation interlayered with siliciclastic deposits and palaeosol profiles. Calcretization is developed over 2–8 m thick layers of coarse deposits (conglomeratic and medium- to coarse-grained sandstone), forming beds that are highly cemented by calcium carbonate. Calcrete beds (lithofacies C) form laterally discontinuous layers traceable for more than 700 m laterally and up to 8 m thick, on average 5 m thick (Figure 7a). Reconstructed geological sections show that calcrete beds reach up to 3 km in extension. They do not occupy a defined stratigraphic position in the Serra da Galga Formation. Instead, they are found at lower, intermediate and upper portions in the stratigraphic unit (Figure 2). Furthermore, the calcrete bodies commonly exhibit upper and lower diffuse transitions with their surrounding deposits. These transitions are marked by a progressive increase in calcium carbonate cementation towards the centre of the calcrete beds.

Interpretation: Calcretization observed in these calcrete beds (lithofacies C) relates to abiotic processes, which mostly occur more effectively when groundwater percolates through deposits of higher permeability (Mann & Horwitz, 1979; Nash & McLaren, 2003; Wright, 2007). In fact, the described calcrete beds show a strong connection to coarse-grained channelized deposits, which corroborates the hypothesis of a phreatic-driven genesis of the calcrete. As a result, calcretes are normally observed occupying the proximal and medial parts of fluvial systems (e.g. Nash & Smith, 1998; Tandon & Narayan, 1981), as described for the Serra da Galga Formation. From this observation it is most likely that these calcrete beds fit the

fourth-type groundwater calcrete described by Alonso-Zarza and Wright (2010). The various stratigraphic levels occupied by the calcrete beds further indicate that repeated episodes of water-table oscillations controlled the post-depositional cementation in the Serra da Galga Formation.

5 | PROPOSAL FOR A NEW LITHOSTRATIGRAPHIC CLASSIFICATION

Two depositional environments can be inferred in the Serra da Galga Formation: (a) a channel-belt environment that is topographically elevated in the alluvial surface and internally displays the amalgamation of types 1 and 2 channel fills; (b) an interchannel environment where unconfined overbank deposits alternate with type 3 channel fills. Palaeosols are ubiquitous features that appear interstratified throughout the entire succession. The Serra da Galga Formation demonstrates a channel-to-interchannel thickness ratio that varies approximately from 7, at the Price 1 type-section, to 2 at the BR050 type-section. This downflow increase in interchannel deposits relates to the fact that cannibalization of overbank deposits by avulsing channels tends to be greater towards fan apices along a distributive fluvial network, according to which channel bodies bifurcate outwards from the proximal zone (Price 1 type-section) to the medial zone (BR050 type-section) in a NNW direction (Dal'Bó, Soares, Basilici, Rodrigues, & Menezes, 2019; Soares et al., 2018; cf. Cain & Mountney, 2009; Hartley, Weissmann, Nichols, & Warwick, 2010; Weissmann et al., 2010). The stratigraphic framework allows to interpret the Serra da Galga Formation as an ancient distributive fluvial system that is unrelated to the adjacent and time-equivalent Marília Formation (Soares et al., 2018; Figure 10). The deposits of the Serra da Galga Formation have historically been assigned to the Marília Formation, subdivided into the Serra da Galga and the Ponte Alta members. Nevertheless, when compared with the Marília Formation, the Serra da Galga Formation does not show compatible lithological, stratigraphic nor genetic resemblance (Figure 11; Table 2). According to the International Code for Stratigraphic Nomenclature (Murphy & Salvador, 1999), a formation is defined primarily on the basis of its lithology and needs to be traceable at the scale of regional geological mapping. In addition, the code requires that a formation shows relative lithological homogeneity and lateral continuity. In this regard, this work emphasizes that the Serra da Galga Formation does present a series of unique characteristics that permit its differentiation from the correlative Marília Formation and consequently to be categorized as a new lithostratigraphic unit. Thereby, this work proposes the establishment of the Serra da Galga Formation as a separate formation for these four main points: (a) lithology, (b) stratigraphic organization, (c) depositional environment, and (d) biostratigraphy.

The in-depth lithological and stratigraphic characterization of the Serra da Galga Formation has revealed a succession that differs markedly from the Marília Formation. The three adopted type-sections (Price 1, BR050, and Lafarge Quarry) display a stratigraphic organization composed of a complex interbedding of large-scale sheet channel

bodies, small-scale crevasse channel fills, interchannel deposits, palaeosols, and large-scale calcrete beds (Figure 10). These sedimentary units are recognized as associated with deposition in the context of a distributive fluvial system.

Conversely, southeastern and northwestern outcropping strata of the Marília Formation display different lithological and stratigraphic organization. The nature of the lateral transition between the Serra da Galga Formation and the Marília Formation is still uncertain, and so as the possible position of a limit (Figure 1) and future studies are required to better constrain the lithostratigraphic boundary between these units. In the southeastern region (Figure 11; Table 2), the Marília Formation is described as a succession characterized by cyclic alternations between sheet-like layers of unconfined flow deposits and palaeosols (Basilici, Dal' Bo, & Oliveira, 2016). The unconfined flow deposits form tabular sheet layers that are limited at the base and the top by erosive surfaces. They extend up to 60 m laterally and 0.1–0.6 m vertically, and are composed of poorly sorted, intraformational conglomeratic sandstones (Basilici, Dal' Bo, & Oliveira, 2016; Soares et al., 1980). The type-section of the Marília Formation was first defined at this southeastern region (Soares et al., 1980). At this location, palaeosol profiles overlay the unconfined flow deposits and correspond up to 95% of the thickness of the unit succession (Basilici, Dal' Bo, & Oliveira, 2016). Palaeosols correspond to Inceptisols and occur as vertically stacked profiles separated by partially preserved deposits (compound palaeosols sensu Morrison, 1978 and Kraus, 1999). The arrangement of unconfined-

flow deposits overprinted by compound palaeosols is interpreted as a flat area at the distal part of a distributive fluvial system where episodes of unconfined floods alternated with pedogenic activity (Basilici, Dal' Bo, & Oliveira, 2016). However, these deposits cannot correspond to the distal counterpart of the Serra da Galga distributive fluvial system as the latter's palaeoflow direction is to northwest.

In the northwestern region (Figure 11; Table 2), the Marília Formation displays interbedding of ephemeral channel deposits, aeolian sand-sheet sandstones and palaeosols. Ephemeral-channel deposits are composed of conglomeratic sandstones that form lenticular beds of concave-up bottom and planar top. Channel bodies are up to 7 km in length, 2 km wide, and up to 4 m thick. Lenses are composed of multi-story strata of poorly-sorted, coarse- to medium-grained sandstone cross-beds, and correspond to ephemeral-channel deposits (Basilici et al., 2009; Basilici & Dal' Bo, 2010; Goldberg & Garcia, 2000). Palaeosols occur as laterally continuous tabular layers of massive sandstone, varying from 0.3 to 1.8 m thick, and correspond to profiles of Aridisols, Alfisols, Vertisols, and Entisols (Basilici et al., 2009; Dal'Bó, Basilici, & Angélica, 2010). The aeolian sand sheet is formed of fine-grained sandstone in tabular layers that extend laterally for more than 50 m and vary in thickness from 0.9 to 15 m. The bottom surface is approximately horizontal whereas the upper boundary is marked by a diffuse transition with the palaeosols. The sandstone is organized in planar horizontal or low-angle laminae and is interpreted as subcritical translent climbing ripples (Basilici et al., 2009; Basilici & Dal' Bo, 2010).

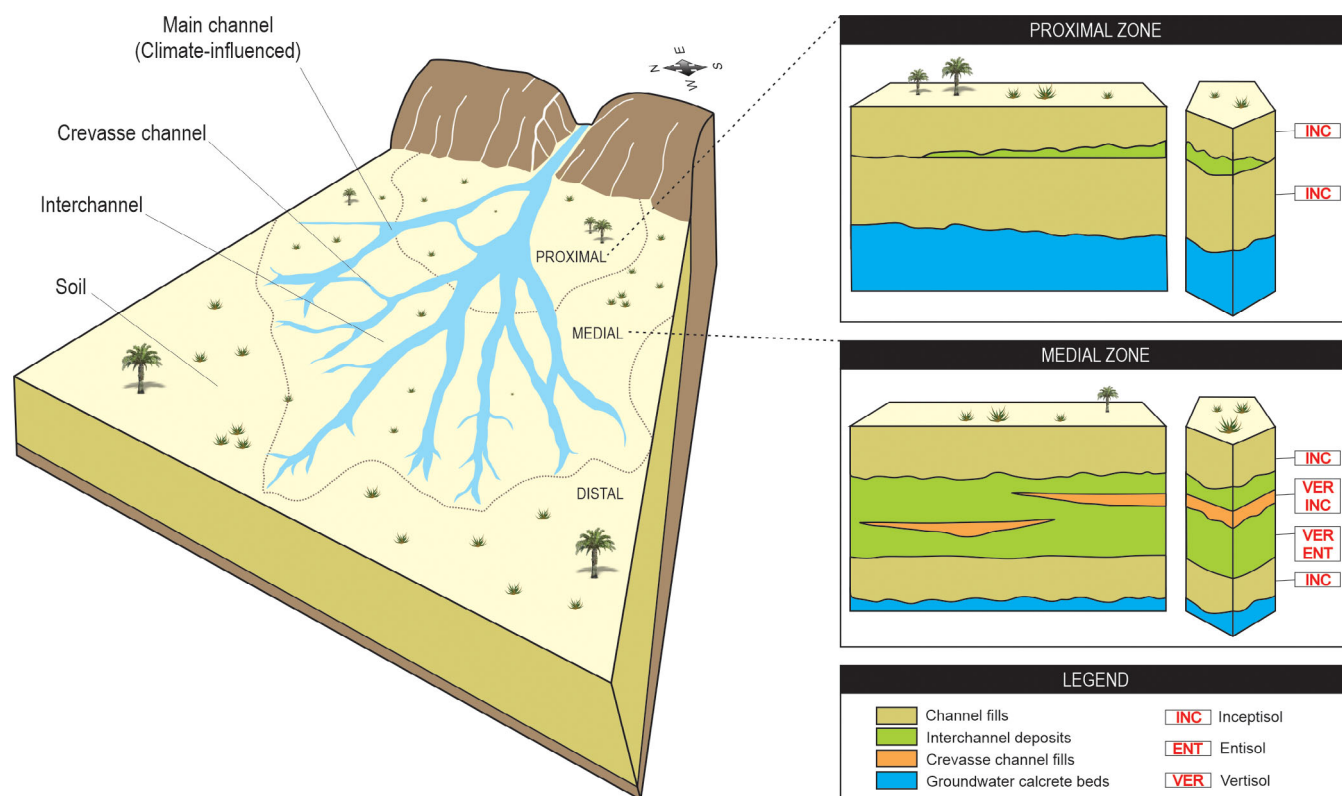


FIGURE 10 Depositional model of the Serra da Galga Formation interpreted as a distributive fluvial system. See text for further explanation [Colour figure can be viewed at wileyonlinelibrary.com]

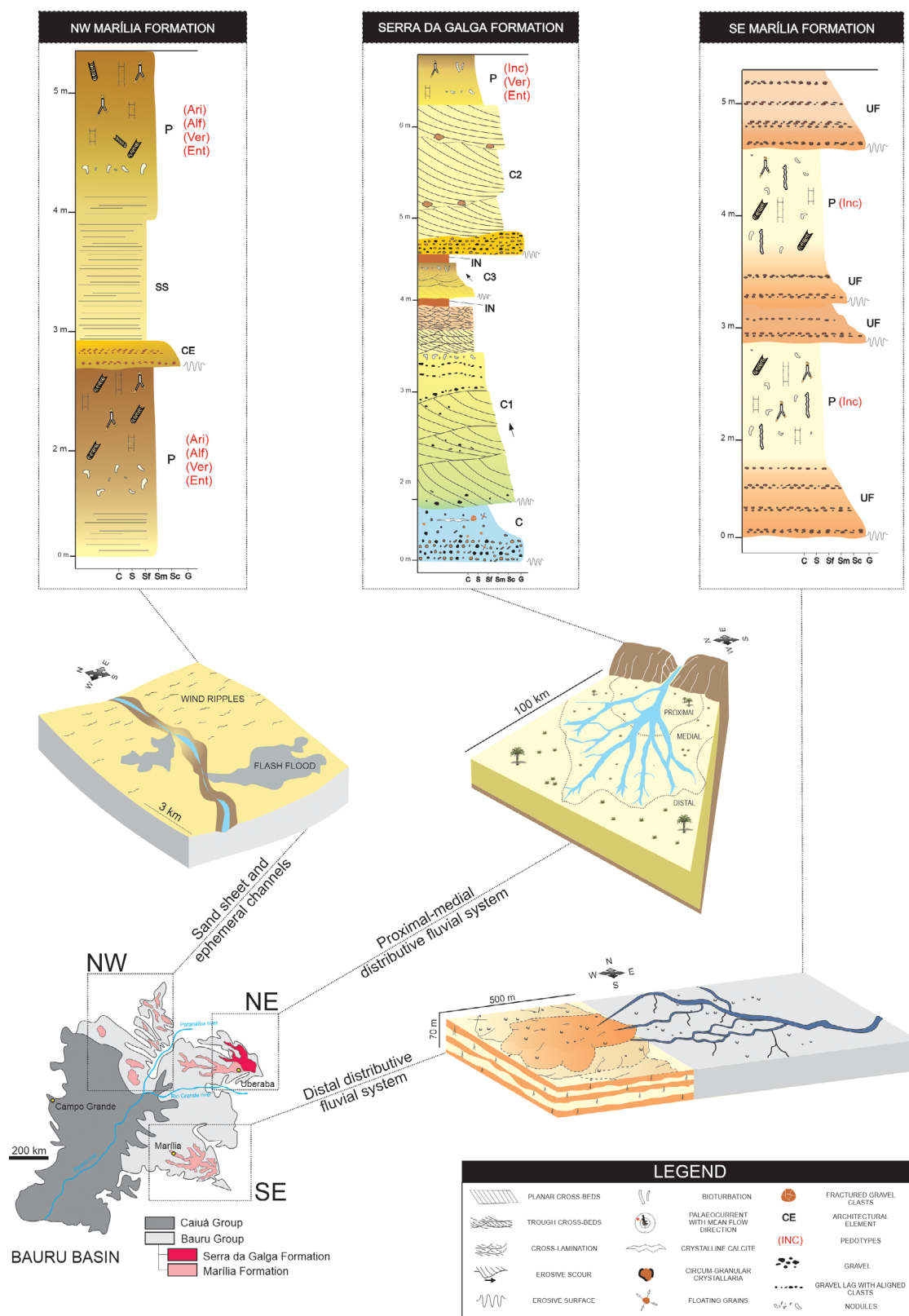


FIGURE 11 Schematic diagram of the contrasting lithostratigraphic and genetic differences between the Serra da Galga Formation and adjacent deposits of the Marília Formation. Lithostratigraphy and depositional models of the Marília Formation at the southeastern region (modified from Basilici, Dal' Bo, & Oliveira, 2016) and northwestern region (modified from Basilici, Dal' Bó, & Ladeira, 2009) and of the Serra da Galga Formation at the northeastern portion of the Bauru Group. Architectural elements are sand sheet [SS], ephemeral channel [CE], type 1 channel fill [C1], type 2 channel fill [C2], type 3 channel fill [C3], interchannel [IN], calcrete beds [C], and unconfined flow deposits [UF]. Palaeosol profiles [P] are further categorized as Inceptisols (Inc), Entisols (Ent), Vertisols (Ver), Aridisols (Ari), and Alfisols (Alf). See text for further explanations [Colour figure can be viewed at wileyonlinelibrary.com]

TABLE 2 Summary of comparative differences between the Marília and the Serra da Galga formations

	Marília Formation	Serra da Galga Formation
Previous nomenclature	Echaporã Member	Serra da Galga and Ponte Alta members
Lithology	Conglomeratic sandstones; poorly-sorted, coarse- to medium-grained cross-bedded sandstones, and fine-grained sandstones.	Sandy conglomerate; planar or trough cross-bedded pebbly sandstone; planar and cross-laminated fine-grained sandstone; fine to muddy sandstone and mudstones.
Stratigraphic organization	Cyclic alternations between sheet-like layers of unconfined flow deposits and Inceptisols at the southeast region; Interbedding of ephemeral channel deposits, aeolian sand-sheet sandstones and palaeosols (Aridisol, Alfisols, Vertisols, and Entisol) at the northwest.	Complex interbedding of large-scale sheet channel fills, small-scale crevasse channel fills, interchannel deposits, large-scale calcrete beds and palaeosols (Inceptisols, Entisols, and Vertisols).
Depositional environment	Flat area at the distal part of a distributive fluvial system at the southeast; ephemeral channels and aeolian sand sheets in the northwest.	Distributive fluvial system with palaeoflow towards northwest.
Fossil content	Theropod (abelisauroids) and sauropod (titanosaurs) dinosaurs, crocodyliforms and ichnofossils. See the Geological Setting for further explanation.	Fishes (e.g., siluriforms, lepisosteiforms, amiids, characiforms, perciforms, and dipnoans), anurans, podocnemidid turtles, squamates (iguanians), mesoeucrocodylians (peirosaurids, itasuchids, 'advanced notosuchians'), theropods (e.g., abelisauroids, maniraptorans, aves), titanosaur sauropods, conchostracans, ostracodans, charophytans, molluscs (gastropods and bivalves) and ichnofossils. See the Geological Setting for further explanation.

In terms of biostratigraphy, correlations between the Serra da Galga and the Marília formations are still unclear. Until now, the fossil record for the Marília Formation was comprised mostly by specimens from the Serra da Galga Formation (e.g., see Martinelli & Teixeira, 2015 and references herein). In contrast, vertebrate remains represented by abelisauroids, titanosaurs, crocodyliforms from the Echaporã Member in the São Paulo State (southeastern region, Figure 11; Table 2) are relatively few; titanosaur remains from the Minas Gerais State (northeastern region, Figure 11; Table 2) have been reported, but are not yet taxonomically positioned, and, as such, cannot be properly correlated with those from the Serra da Galga Formation (e.g., Bertini et al., 2001; Iori & Arruda-Campos, 2016; Méndez et al., 2014; Riff, Costa, & Machado, 2013). The only genus occurring in both units is the bivalvian *Anodontites*, but with different species between these units (Ghilardi et al., 2011; Ragonha & Mezzalana, 1985), and probably representing different ages. Regarding the crocodyliforms, the best-known fossil group from the Bauru Basin, the only fossil described for the Echaporã Member (Marília Formation) is a partial skull roof with affinities to *Itasuchus* and peirosaurids (Iori & Arruda-Campos, 2016). Peirosaurids and crocodyliforms closely related to *Itasuchus* also occur in the Adamantina Formation, as well as in the Marília and Serra da Galga formations (e.g., Carvalho, Vasconcellos, & Tavares, 2007; Pinheiro et al., 2018; Price, 1955). Consequently, these crocodyliforms are not appropriate for biostratigraphic purposes. The same holds true for theropod and sauropod dinosaurs, which are still poorly represented in the Marília Formation, as here proposed.

Based on the exposed lithological, stratigraphic, genetic and biostratigraphic differences, this work proposes to reclassify and elevate the Serra da Galga succession, previously referred to in the literature as a member, to the formation rank. In addition, the groundwater calcrete beds, previously referred as the Ponte Alta Member, are recognized as part of the Serra da Galga Formation. These sedimentary bodies, even though they possess homogeneous lithological characteristics throughout the unit, based on the International Code for Stratigraphic Nomenclature (Murphy & Salvador, 1999), should not be considered a member, as (a) they do not occupy a defined stratigraphic position, and (b) they are arranged in an intricate framework of layers in which lateral or vertical traceability is unsuitable for regional mapping. Thereby, this work proposes to deprecate the Ponte Alta Member classification and to refer the groundwater calcrete beds as undifferentiated bodies of the Serra da Galga Formation. Finally, this proposal is tied to the sedimentary interpretation of the NE part of Bauru Group and permits to unravel the geological history of this area. For that, we believe, that this proposed lithostratigraphic revision offers a logical and practical alternative to the previous stratigraphic organization of the NE part of Bauru Group.

6 | CONCLUSIONS

This work proposes a new classification of the upper portion of the Bauru Group at the northeastern margin of the Bauru Basin. The sedimentary succession corresponding to the Serra da Galga and Ponte Alta members of the Marília Formation was described in detail and

reclassified as Serra da Galga Formation. This work has used an in-depth sedimentological, palaeopedological, and stratigraphic analysis to demonstrate how the northeastern sedimentary succession of the upper portion of the Bauru Group differs from its adjacent occurrences of the Marília Formation and proposes a different lithostratigraphic model for the northeastern margin of the basin. The lithostratigraphic characterization of the Serra da Galga Formation was conducted at three adopted type-sections: Price 1, Lafarge Quarry, and BR050 sites. In this formation, eleven sedimentary facies and three pedotypes were identified and assigned to six architectural elements. The sedimentary succession was mapped and organized in a stratigraphic framework composed of larger channel deposits (types 1 and 2 channel fills) interbedded with smaller crevasse channel fills (type 3 channel fills), interchannel deposits, palaeosols, and groundwater calcrete beds. This work interpreted the northeastern deposits as an ancient distributive fluvial system characterized by a proximal zone (Price 1 and Lafarge Quarry type-sections) and a medial zone (BR050 type-section) along which the distributive fluvial system displays a clear downstream decrease in channel-to-interchannel ratio as a result of probable downflow bifurcation of channel bodies towards the NNW. Finally, based on the marked lithological, stratigraphic, palaeopedological, biostratigraphic, and genetic characteristics of this sedimentary succession, this work proposes a new lithostratigraphic classification for the upper portion of the northeastern deposits of the Bauru Group, previously referred to as the Serra da Galga and Ponte Alta members, elevating the succession to formation level as the Serra da Galga Formation. The Ponte Alta Member is discontinued, and its strata are considered instead, as part of the Serra da Galga Formation, in view of their poor traceability and suitability for regional geological mapping.

ACKNOWLEDGEMENTS

The authors thank the São Paulo Research Foundation - FAPESP (grant no. 2018/10574-8; project no. 2012/23209-0), Minas Gerais Research Foundation - FAPEMIG (APQ-02194-15) and the National Council for Scientific and Technological Development - CNPq (project no 474227/2013-8; 310164/2015-0; 305098/2018-7) for sustaining the scientific activities of the first, second, and third authors. The Complexo Cultural e Científico de Peirópolis (CCCCP-UFTM) is thanked for providing support during field data collection. The authors also thank Karin Goldberg, the anonymous referees and the Chief Editor, Ian Somerville, for their support and valuable inputs that have significantly improved this manuscript.

ORCID

Marcus Vinícius Theodoro Soares  <https://orcid.org/0000-0002-8618-7210>

Giorgio Basili  <https://orcid.org/0000-0003-2801-9013>

REFERENCES

- Almeida, F. F. M., & Barbosa, O. (1953). *Geologia das quadriculas de Piracicaba e Rio Claro, Estado de São Paulo* (Vol. 143, p. 96). Rio de Janeiro: Departamento Nacional de Produção Mineral.

- Alonso-Zarza, A. M., & Wright, V. P. (2010). Calcretes. In A. M. Alonso-Zarza & L. H. Tanner (Eds.), *Carbonates in continental settings: Facies, environments and processes* (Vol. 61, pp. 225–267). Amsterdam, the Netherlands: *Developments in Sedimentology*, Elsevier.
- Arai, M., & Dias-Brito, D. (2018). The Ibaté paleolake in SE Brazil: Record of an exceptional late Santonian palynoflora with multiple significance (chronostratigraphy, paleoecology and paleophytogeography). *Cretaceous Research*, 84, 264–285.
- Báez, A. M., Gomez, R. O., Ribeiro, L. C. B., Martinelli, A. G., Teixeira, V. P. A., & Ferraz, M. L. F. (2012). The diverse Cretaceous neobatrachian fauna of South America: *Uberabatrachus carvalhoi*, a new frog from the Maastrichtian Marília formation, Minas Gerais, Brazil. *Gondwana Research*, 22, 1141–1150. <https://doi.org/10.1016/j.gr.2012.02.021>.
- Banham, S. G., & Mountney, N. P. (2014). Climatic versus halokinetic control on sedimentation in a dryland fluvial succession: Triassic Moenkopi Formation, Utah, USA. *Sedimentology*, 61, 570–608.
- Barcelos, J. H. (1984). *Reconstrução paleogeográfica da sedimentação do Grupo Bauru baseada na sua redefinição estratigráfica parcial em território paulista e no estudo preliminar for a do Estado de São Paulo*. Inst. de Geociências e Ciências Exatas, Universidade Estadual Paulista, Rio Claro, Tese de Livre-Docência, 90.
- Basili, G., Dal' Bo, P. F., & Oliveira, E. F. (2016). Distribution of palaeosols and deposits in the temporal evolution of a semiarid fluvial distributary system (Bauru Group, Upper Cretaceous, SE Brazil). *Sedimentary Geology*, 341, 245–264.
- Basili, G., & Dal' Bo, P. F. F. (2010). Anatomy and controlling factors of a Late Cretaceous Aeolian sand sheet: The Marília and the Adamantina formations, NW Bauru Basin, Brazil. *Sedimentary Geology*, 226, 71–93.
- Basili, G., Dal' Bó, P. F. F., & Ladeira, F. S. (2009). Climate-induced sediment-palaeosol cycles in a Late Cretaceous dry aeolian sand sheet: Marília Formation (North-West Bauru Basin, Brazil). *Sedimentology*, 56, 1876–1904.
- Basili, G., Fiorelli, L. E., & Dal' Bo, P. F. (2016). Comment on "Evolution and palaeoenvironment of the Bauru Basin (Upper Cretaceous, Brazil)" by Luiz Alberto Fernandes and Claudia Maria Magalhaes Ribeiro. *Journal of South American Earth Sciences*, 91(389–393), 1–5. <https://doi.org/10.1016/j.jsames.2016.06.015>.
- Basili, G., Sgarbi, G. N., & Dal Bó, P. F. F. (2012). A Sub-Bacia Bauru: Um Sistema continental entre deserto e cerrado. In Y. Hasui, C. D. R. Carneiro, F. F. M. Almeida, & A. Bartorelli (Eds.), *Geologia do Brasil* (pp. 520–543). São Paulo, Brasil: Beca Produções Culturais.
- Bertini, R. J., Santucci, R. M., & Arruda-Campos, A. C. (2001). Titanossauros (Sauropoda: Saurischia) no Cretáceo Superior continental (Formação Marília, Membro Echaporã) de Monte Alto, estado de São Paulo, e correlação com formas associadas do Triângulo Mineiro. *Geociências*, 20, 93–103.
- Brito, R. J., Amaral, C. R. L., & Machado, L. P. (2006). A ictiofauna do Grupo Bauru, Cretáceo Superior da Bacia Bauru, sudeste do Brasil. In V. Gallo, P. M. Brito, H. M. Silva, & F. J. Figueroa (Eds.), *Paleontologia de vertebrados: Grandes temas e contribuições científicas* (pp. 133–143). Rio de Janeiro, Brasil: Editora Interciência.
- Brookfield, M. E. (1977). The origin of bounding surfaces in ancient aeolian sandstones. *Sedimentology*, 24, 303–332.
- Buczynski, C., & Chafetz, H. S. (1987). Siliciclastic grain breakage and displacement due to carbonate crystal growth: An example from the Lenders Formation, Permian of North Central Texas, USA. *Sedimentology*, 34, 837–843.
- Burns, C. E., Mountney, N. P., Hodgson, D. M., & Colomera, L. (2017). Anatomy and dimensions of fluvial crevasse-splay deposits: Examples from the Cretaceous Castlegate sandstone and Neslen formation, Utah, USA. *Sedimentary Geology*, 351, 21–35.
- Cain, S. A., & Mountney, N. P. (2009). Spatial and temporal evolution of a terminal fluvial fan system: The Permian Organ Rock Formation, South-east Utah, USA. *Sedimentology*, 56, 1774–1800.

- Campos, D. A., Kellner, A. W. A., Bertini, R. J., & Santucci, R. M. (2005). On a titanosaurid (Dinosauria, Sauropoda) vertebral column from the Bauru Group, Late Cretaceous of Brazil. *Arquivos do Museu Nacional*, 63, 565–593.
- Carbonaro, F. A., Rohn, R., & Ghilardo, R. P. (2013). Conchostráceos *Palaeolimnadiopsis* (Spinicaudata, Crustacea) do Grupo Bauru (Cretáceo Superior, Bacia Bauru): Taxonomia, paleoecologia e paleobiogeografia. *Revista Brasileira de Paleontologia*, 16(2), 283–296.
- Carvalho, I. S., Ribeiro, L. C. B., & Avilla, L. S. (2004). *Uberabasuchus terrificus* sp. nov., a new Crocodylomorpha from the Bauru Basin (Upper Cretaceous), Brazil. *Gondwana Research*, 7, 975–1002.
- Carvalho, I. S., Vasconcellos, F. M., & Tavares, S. A. S. (2007). *Montealtosuchus arrudacamposi*, a new peirosaurid crocodile (Mesoeucrocodylia) from the Late Cretaceous Adamantina Formation of Brazil. *Zootaxa*, 1607, 35–46.
- Catt, J. A. (1990). Paleopedology manual. *Quaternary International*, 6, 1–95.
- Chakraborty, C., & Bose, P. K. (1992). Ripple/dune to upper stage plane bed transition: Some observations from the ancient record. *Geological Journal*, 27, 349–359.
- Collinson, J. D., & Mountney, N. P. (2019). *Sedimentary structures* (4th ed., p. 340). Edinburgh, Scotland: Dunedin Academic Press.
- Coronel, M. D., Isla, M. F., Veiga, G. D., Mountney, N. P., & Colomera, L. (2020). Anatomy and facies distribution of terminal lobes in ephemeral fluvial successions: Jurassic Tordillo Formation, Neuquén Basin, Argentina. *Sedimentology*, 67, 2596–2624. <https://doi.org/10.1111/sed.12712>.
- Costa, J. E. (1988). Rheologic, geomorphic and sedimentologic differentiation of water floods, hyperconcentrated flows and debris flows. In V. R. Baker, R. C. Kochel, & P. C. Patton (Eds.), *Flood geomorphology* (pp. 113–122). Chichester, England: John.
- Coutinho, J. M. V., Coimbra, A. M., Brandt Neto, M., & Rocha, G. A. (1982). Lavas alcalinas analcímicas associadas ao Grupo Bauru (Kb) no Estado de São Paulo, Brasil. *Congresso Latinoamericano de Geologia*, 5(2), 185–196.
- Dal'Bó, P. F., Soares, M. V. T., Basilici, G., Rodrigues, A. G., & Menezes, M. N. (2019). Spatial variations in distributive fluvial system architecture of the Upper Cretaceous Marília Formation, SE Brazil. *Geological Society, London, Special Publications*, 488, SP488–SP486.
- Dal'Bó, P. F. F., Basilici, G., & Angélica, R. S. (2010). Factors of palaeosol formation in a Late Cretaceous eolian sand sheet paleoenvironment, Marília Formation, southeastern Brazil. *Palaeogeography, Palaeoclimatology, Palaeoecology*, 292, 349–365.
- Dias-Brito, D., Musacchio, E. A., Castro, J. C., Maranhão, M. S. A., Suárez, J. M., & Rodrigues, R. (2001). Grupo Bauru: Uma unidade continental do Cretáceo do Brasil – Concepções baseadas em dados micropaleontológico, isotópicos e estratigráficos. *Revue de Paléobiologie*, 20, 245–304.
- Fernandes, L. A. (1992). *A cobertura cretácea suprabasáltica no Paraná e Pontal do Paranapanema (SP): Os grupos Bauru e Caiuá* (pp. 1–129). Dissertação de Mestrado, IGc/USP, São Paulo.
- Fernandes, L. A., & Coimbra, A. M. (1994). O Grupo Caiuá (Ks): Revisão estratigráfica e contexto deposicional. *Revista Brasileira de Geociências*, 24(3), 164–176.
- Fernandes, L. A., & Coimbra, A. M. (2000). Revisão estratigráfica da parte oriental da Bacia Bauru (Neocretáceo). *Revista Brasileira de Geociências*, 30(4), 717–728.
- Francischini, H., Paes Neto, V. D., Martinelli, A. G., Pereira, V. P., Marinho, T. S., Teixeira, V. P. A., ... Schultz, C. L. (2016). Invertebrate traces in pseudo-coprolites from the Upper Cretaceous Marília Formation (Bauru Group), Minas Gerais State, Brazil. *Cretaceous Research*, 57, 29–39. <https://doi.org/10.1016/j.cretres.2015.07.016>.
- Fregenal-Martínez, M., Meléndez, N., Muñoz-García, M. B., Elez, J., & Horra, R. (2017). The stratigraphic record of the Late Jurassic–Early Cretaceous rifting in the Alto Tajo-Serranía de Cuenca region (Iberian Ranges, Spain): Genetic and structural evidences for a revision and a new lithostratigraphic proposal. *Revista de la Sociedad Geológica de España*, 30(1), 113–142.
- Fulfaro, V. J., Etchebehere, M. L. D. C., Perinotto, J. A. J., & Saad, A. R. (1999). Santo Anastácio: Um Geossolo Cretácico na Bacia Caiuá. In D. Dias-Brito (Ed.), *Simpósio Sobre o Cretáceo do Brasil, 5 e Simpósio sobre el Cretácico de América del Sur* (pp. 125–130). Boletim: Serra Negra.
- Ghilardi, R. P., D'Agosta, F. C. P., Alves, K., & Arruda-Campos, A. C. (2011). Tafonomia de moluscos fósseis do Grupo Bauru (Cretáceo Superior, Bacia Bauru) na região do município de Monte Alto, São Paulo, Brasil. *Boletim do Museu Paraense Emílio Goeldi*, 6, 197–206.
- Goldberg, K., & Garcia, A. J. V. (2000). Palaeobiogeography of the Bauru Group, a dinosaur-bearing Cretaceous unit, northeastern Paraná Basin, Brazil. *Cretaceous Research*, 21, 241–254.
- Harms, J. C., Southard, J. B., & Walker, R. G. (1982). Structures and sequences in clastic rocks. *Society of Economic Paleontologists and Mineralogists Short Course* (No. 9).
- Hartley, A. J., Weissmann, G. S., Nichols, G. J., & Warwick, G. L. (2010). Large distributive fluvial systems: Characteristics, distribution, and controls on development. *Journal of Sedimentary Research*, 80, 167–183.
- Hubert, J. F., & Hyde, M. G. (1982). Sheet-flow deposits of graded beds and mudstones on an alluvial sandflat-playa system: Upper Triassic Blomidon redbeds, St Mary's Bay, Nova Scotia. *Sedimentology*, 29, 457–474.
- Iori, F. V., & Arruda-Campos, A. C. A. (2016). Os crocodiliformes da Formação Marília (Bacia Bauru, Cretáceo Superior) na região de Monte Alto, estado de São Paulo, Brasil. *Revista Brasileira de Paleontologia*, 19 (3), 537–546.
- Jopling, A. V. (1965). Hydraulic factors and shape of laminae. *Journal of Sedimentary Petrology*, 35, 777–791.
- Jopling, A. V., & Walker, R. G. (1968). Morphology and origin of ripples-drift cross-lamination, with examples from the Pleistocene of Massachusetts. *Journal of Sedimentary Petrology*, 38, 971–984.
- Kellner, A. W. A., Campos, D. A., & Trotta, M. N. F. (2005). Description of a titanosaurid caudal series from the Bauru Group, Late Cretaceous of Brazil. *Arquivos do Museu Nacional*, 63, 529–564.
- Kellner, A. W. A., Figueiredo, R. G., Azevedo, S. A. K., & Campos, D. A. (2011). A new Cretaceous notosuchian (Mesoeucrocodylia) with bizarre dentition from Brazil. *Zoological Journal of the Linnean Society*, 163, 109–115.
- Kraus, M. J. (1999). Paleosols in clastic sedimentary rocks: Their geologic applications. *Earth-Science Reviews*, 47, 41–70.
- Lunt, I. A., Bridge, J. S., & Tye, R. S. (2004). Development of a 3-D depositional model of a braided-river gravels and sands to improve aquifer characterization. In J. S. Bridge & D. W. Hyndman (Eds.), *Aquifer characterization* (pp. 139–169). Tulsa, OK: SEPM Society for Sedimentary Geology Special Publication.
- Magalhães Ribeiro, C. M. (2002). Ovo e fragmentos de cascas de ovos de dinossauros, provenientes de região de Peirópolis, Uberaba, Minas Gerais. *Arquivos do Museu Nacional*, 60, 223–228.
- Mann, A. W., & Horwitz, R. C. (1979). Groundwater calcrete deposits in Australia: Some observations from Western Australia. *Journal of the Geological Society of Australia*, 26, 293–303.
- Martinelli, A. G., Basilici, G., Fiorelli, L. E., Carolina, K. C., Karfunkele, J., Ariela Costa Diniz, A. C., ... Marinho, T. S. (2019). Palaeoecological implications of an Upper Cretaceous tetrapod burrow (Bauru Basin; Peirópolis, Minas Gerais, Brazil). *Palaeogeography, Palaeoclimatology, Palaeoecology*, 528, 147–159. <https://doi.org/10.1016/j.palaeo.2019.05.015>.
- Martinelli, A. G., Bogan, S., Agnolin, F. L., Ribeiro, L. C. B., Cavellani, C. L., Ferraz, M. L. F., & Teixeira, V. P. A. (2013). First fossil record of amiid fishes (Halecomorphi, Amiiformes, Amiidae) from the Late Cretaceous of Uberaba, Minas Gerais State, Brazil. *Alcheringa: An Australasian Journal of Palaeontology*, 37, 105–113.

- Martinelli, A. G., & Teixeira, V. P. A. (2015). The Late Cretaceous vertebrate record from the Bauru Group in the Triângulo Mineiro, southeastern Brazil. *Boletín Geológico y Minero*, 126(1), 129–158.
- Méndez, A. H., Novas, F. E., & Iori, F. V. (2014). New record of abelisauroid theropods from the Bauru Group (Upper Cretaceous), São Paulo State, Brazil. *Revista Brasileira de Paleontologia*, 17, 23–32. <https://doi.org/10.4072/rbp.2014.1.03>.
- Miall, A. D. (1978). Lithofacies types and vertical profile models in braided river deposits: A summary. In: *Fluvial Sedimentology* (Ed. A.D. Miall), Canadian Society of Petroleum Geologists. *Memoir. Canadian Society of Petroleum Geologists*, 5, 597–604.
- Miall, A. D. (1985). Architectural-element analysis: A new method of facies analysis applied to fluvial deposits. *Earth-Science Reviews*, 22, 261–308.
- Miall, A. D. (2006). *The geology of fluvial deposits: Sedimentary facies, basin analysis and petroleum geology*. Berlin: Springer.
- Miall, A. D. (2016). *Stratigraphy: A modern synthesis* (pp. 1–454). Berlin: Springer-Verlag.
- Mineiro, A. S., & Santucci, R. M. (2018). Ichnofabrics and ichnofossils from the continental deposits of the Serra da Galga Member, Marília Formation, Bauru Group (Upper Cretaceous), Uberaba, Minas Gerais, Brazil. *Journal of South American Earth Sciences*, 86, 287–300.
- Mineiro, A. S., Santucci, R. M., Da Rocha, D. M. S., De Andrade, M. B., & Nava, W. R. (2017). Invertebrate ichnofossils and rhizoliths associated with rhizomorphs from the Marília Formation (Echaporã Member), Bauru Group, Upper Cretaceous, Brazil. *Journal of South American Earth Sciences*, 80, 529–540.
- Mohr, E. C. J., Van Baren, F. A., & Van Schuylenborgh, J. (1972). *Tropical soils*. The Hague: Mouton.
- Morrison, R. B. (1978). Quaternary soil stratigraphy – Concepts, methods, and problems. In W. C. Mahaney (Ed.), *Quaternary soils* (pp. 77–108). Norwich: Geo-Abstracts.
- Murphy, M. A., & Salvador, A. (1999). International stratigraphic guide – An abridged edition. *Episodes*, 22, 255–271.
- Nash, D. J., & McLaren, S. J. (2003). Kalahari valley calcretes: Their nature, origins and environmental significance. *Quaternary International*, 111, 3–22.
- Nash, D. J., & Smith, R. G. (1998). Multiple calcrete profiles in the Tabernas Basin, Southeast Spain: Their origins and geomorphic implications. *Earth Surface Processes and Landforms*, 23, 1009–1029.
- Nemec, W., & Steel, R. J. (1984). Alluvial and coastal conglomerates: Their significant features and some comments on gravelly mass-flow deposits. In E. H. Koster & R. J. Steel (Eds.), *Sedimentology of gravels and conglomerates* (Vol. 10, pp. 1–31). Calgary, Canada: Canadian Society of Petroleum Geologists Memoir.
- Netterberg, F. (1969). The interpretation of some basin calcrete types. *South Africa Archaeology Bulletin*, 24, 117–122.
- Nichols, G. J., & Fisher, J. A. (2007). Processes, facies and architecture of fluvial distributary system deposits. *Sedimentary Geology*, 195, 75–90.
- Novas, F. E., Carvalho, I. S., Ribeiro, L. C. B., & Méndez, A. H. (2008). First abelisauroid bone remains from the Maastrichtian Marília Formation, Bauru Group, Brazil. *Cretaceous Research*, 29, 625–635.
- Novas, F. E., Ribeiro, L. C. R., & Carvalho, I. S. (2005). Maniraptoran theropod ungual from the Marília Formation (Upper Cretaceous), Brazil. *Revista del Museo Argentino de Ciencias Naturales "Bernardino Rivadavia"*, 7, 31–36.
- Paes Neto, V. D., Francischini, H., Martinelli, A. G., Marinho, T. S., Ribeiro, L. C. B., Soares, M. B., & Schultz, C. L. (2018). Bioerosion traces on titanosaur bones of the Upper Cretaceous Marília Formation of Brazil. *Alcheringa*, 42(3), 415–426.
- Paola, C., Wiele, S. M., & Reinhart, M. A. (1989). Upper-regime parallel lamination as the result of turbulent sediment transport and low amplitude bed forms. *Sedimentology*, 36, 47–59.
- Paula e Silva, F., Chang, H. K., & Caetano-Chang, M. R. (2003). Perfis de referência do Grupo Bauru (K) no Estado de São Paulo. *Geociências*, 22, 21–32.
- Paula e Silva, F., Chang, H. K., & Caetano-Chang, M. R. (2005). Estratigrafia de subsuperfície do Grupo Bauru (K) no Estado de São Paulo. *Revista Brasileira de Geociências*, 35(1), 77–88.
- Paula e Silva, F., Chang, H. K., & Caetano-Chang, M. R. (2009). Sedimentation of the Cretaceous Bauru Group in São Paulo, Paraná Basin, Brazil. *Journal of South American Earth Sciences*, 28, 25–39.
- Paula e Silva, F., Chang, H. K., Caetano-Chang, M. R., & Stradioto, M. R. (2006). Sucessão sedimentar do Grupo Bauru na região de Pirapozinho (SP). *Geociências*, 25(1), 17–26.
- Pimentel, N. L., Wright, V. P., & Azevedo, T. M. (1996). Distinguishing early groundwater alteration effects from pedogenesis in ancient alluvial basins: examples from the Palaeogene of Portugal. *Sedimentary Geology*, 105, 1–10.
- Pinheiro, A. E. P., Pereira, P. V. L. G. C., de Souza, R. G., Brum, A. S., Lopes, R. T., Machado, A. S., ... Simbras, F. M. (2018). Reassessment of the enigmatic crocodyliform "Goniopholis" paulistanus Roxo, 1936: Historical approach, systematic, and description by new materials. *PLoS One*, 13(8), e0199984. <https://doi.org/10.1371/journal.pone.0199984>.
- Price, L. I. (1955). Novos crocodilídeos dos arenitos da Série Bauru, Cretáceo do estado de Minas Gerais. *Anais da Academia Brasileira de Ciências*, 27, 487–498.
- Ragonha, E. W., & Mezzalana, S. (1985). Nova malacofauna dulciaquícola no grupo Bauru (K Sup.) de Monte Alto (SP), Brasil. In *Congresso Brasileiro De Paleontologia. Boletim de Resumos* (pp. 1–70). Fortaleza, Brasil: Boletim de Resumos.
- Retallack, G. J. (1988). Field recognition of paleosols. In J. Reinhardt & W. R. Sigleo (Eds.), *Paleosols and weathering through geologic time: Techniques and applications* (Vol. 216, pp. 1–20). Boulder, CO: Geological Society of America, Special Paper.
- Riff, D., Costa, A. C. S., & Machado, E. B. (2013). New information on Titanosauridae remains (Dinosauria, Sauropoda) from the Marília Formation (Maastrichtian, Bauru Basin) of Campina Verde, Minas Gerais State, Brazil. 73rd Meeting of the Society of Vertebrate Paleontology, Los Angeles. *Journal of Vertebrate Paleontology, Program and Abstracts*, 1, 199–199.
- Rodgers, J. (1954). Nature, usage, and nomenclature of stratigraphic units: A minority report. *Bulletin of the American Association of Petroleum Geologists*, 38(4), 655–659.
- Salgado, L., & Carvalho, I. S. (2008). *Uberabatitan ribeiroi*, a new titanosaur from the Marília Formation (Bauru Group, Upper Cretaceous), Minas Gerais, Brazil. *Palaeontology*, 51, 881–901.
- Santucci, R. M. (2013). *Brazilian titanosaurs*. Brazilian Dinosaur Symposium, 1, Abstract Book, 18.
- Schokker, J., Weerts, H. J. T., Westerhoff, W. E., Berendsen, H. J. A., & Otter, C. (2007). Introduction of the Bostel Formation and implications for the Quaternary lithostratigraphy of The Netherlands. *Netherlands Journal of Geosciences*, 86(3), 197–210.
- Smith, N. D. (1972). Some sedimentological aspects of planar cross-stratification in a Sandy braided river. *Journal of Sedimentary Petrology*, 42(3), 624–634.
- Soares, M. V. T., Basilici, G., Dal' Bó, P. F., Marinho, T. S., Mountney, N. P., Colombero, L., ... Silva, K. E. B. (2018). Climatic and geomorphologic cycles in a semiarid distributive fluvial system, Upper Cretaceous, Bauru Group, SE Brazil. *Sedimentary Geology*, 372, 75–95.
- Soares, P. C., Landim, P. M. B., Fúlfaro, V. J., & Sobreiro Neto, A. F. (1980). Ensaio de caracterização do Cretáceo no Estado de São Paulo: Grupo Bauru. *Revista Brasileira de Geociências*, 10(3), 177–185.
- Soil Survey Staff. (2014). *Keys to soil taxonomy* (12th ed.). Washington, DC: USDA-Natural Resources Conservation Service.
- Tandon, S. K., & Narayan, D. (1981). Calcrete conglomerate, case-hardened conglomerate and concretion: A comparative account of

- pedogenic and non-pedogenic carbonates from the continental Siwalik Group, Punjab, India. *Sedimentology*, 28, 353–367.
- Walker, R. G. (2006). Facies models revisited: Introduction. In H. W. Posamentier & H. G. Walker (Eds.), *Facies models revisited* (Vol. 84, pp. 5–22, 22). Tulsa, OK: SEPM Special Publication.
- Washburne, C. W. (1930). *Petroleum Geology of the State of São Paulo*. Geológico: Inst. Geogr.
- Weissmann, G. S., Hartley, A. J., Nichols, G. J., Scuderi, L. A., Olson, M., Buehler, H., & Banteah, R. (2010). Fluvial form in modern continental sedimentary basins: Distributive fluvial systems. *Geology*, 38, 39–42.
- Wright, V. P. (1990). A micromorphological classification of fossil and recent calcic and petrocalcic microstructures. In L. A. Douglas (Ed.), *Soil micromorphology: A basic and applied science. Developments in Soil Science* (Vol. 19, pp. 401–407). Amsterdam, the Netherlands: Elsevier.
- Wright, V. P. (2007). Calcretes. In D. Nash & S. McLaren (Eds.), *Geochemical sediments and landscapes* (pp. 10–45). Oxford, England: Wiley-Blackwell.
- Wright, V. P., & Tucker, M. E. (1991). Calcretes: An introduction. In V. P. Wright & M. Tucker (Eds.), *Calcretes* (Vol. 2, pp. 1–1222). Oxford, England: Blackwell Scientific Publications.
- Young, A. (1976). *Tropical soils and soil survey*. Cambridge, England: Cambridge University Press.

How to cite this article: Soares MVT, Basilici G, da Silva Marinho T, et al. Sedimentology of a distributive fluvial system: The Serra da Galga Formation, a new lithostratigraphic unit (Upper Cretaceous, Bauru Basin, Brazil). *Geological Journal*. 2021;56:951–975. <https://doi.org/10.1002/gj.3987>